APPLICATION OF WATER CHANNEL - COMPRESSIBLE GAS ANALOGIES TO A PROBLEM OF SUPERSONIC BIPLANE DESIGN

A THESIS

Presented to

The Faculty of the Division of Graduate Studies

Georgia Institute of Technology

In Partial Fulfillment

of the Requirements for the Degree

Master of Science in Aeronautical Engineering

by

Ira Payne Jones, Jr.

November 1950

Cleveland

APPLICATION OF WATER CHANNEL-COMPRESSIBLE GAS ANALOGIES TO A PROBLEM OF SUPERSONIC BIPLANE DESIGN

Approved:

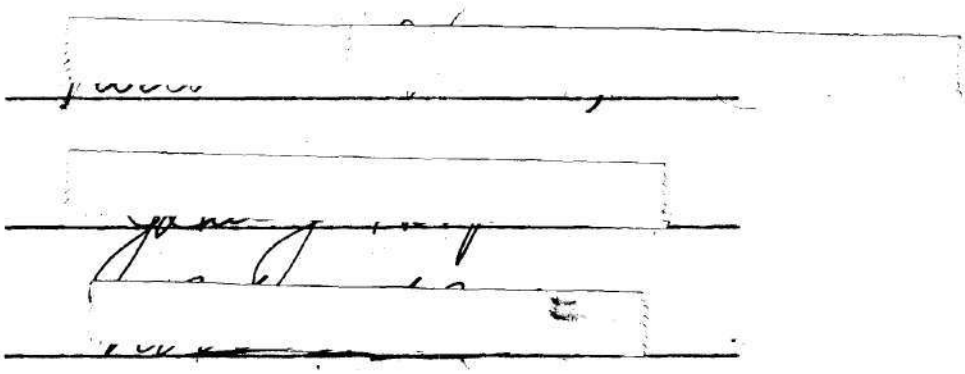

Date Approved by Chairman November 18, 1950

ACKNOWLEDGEMENTS

I take this opportunity to express my deepest appreciation to Mr. H. W. LaVier for his valuable assistance and interest which led to the completion of this project. A word of thanks to the reading committee composed of Mr. H. W. S. LaVier, Mr. J. J. Harper, and Mr. R. L. Allen; and to the staff members of the Daniel Guggenheim School of Aeronautics for their advice and suggestions. Thanks also to the shop personnel who assisted in the construction of the model.

TABLE OF CONTENTS

LIST OF TABLES

LIST OF FIGURES

FIGURE PAGE

APPLICATION OF WATER CHANNEL-COMPRESSIBLE GAS ANALOGIES TO A PROBLEM OF SUPERSONIC BIPLANE DESIGN

SUMMARY

A supersonic biplane design of the Busemann type was tested in the Georgia Institute of Technology twenty foot by four foot water channel at $M=2.03$, over a range of angles of attack and Gap ratios. The water depth distributions were obtained by the probe method. By the application of the hydraulic analogy, pressure distributions and subsequent lift and drag coefficients were obtained. The results compared well with theory and wind tunnel data where such a comparison was possible. An evaluation of the efficiency of the biplane was made as compared to a similar single profile. Within limits, the biplane proved more efficient than the single profile.

INTRODUCTION

It has been shown that an analogy exists between water flow with a free surface, and two-dimensional compressible gas flow. The results of experimental work has indicated that use of the analogy in the transonic and supersonic speed range will yield data of a quantitative and qualitative nature which can be compared closely with theory and wind tunnel results.

The first mathematical basis for the analogy was presented by Riabouchinsky.[1] Further early studies were made by Binnie and Hooker,[2] employing the use of a laval nozzle. The hydraulic analogy as it is used currently was conclusively validated by Preiswerk.[3] Use of the analogy in this country was along experimental applications and was first investigated by the National Advisory Committee for Aeronautics[4] and North American Aviation, Inc.[5] Recent studies on the validity of the hydraulic

---

[1] D. Riabouchinsky, "Mecanique des fluides," Comptes Rendus, 195:998-999, 1932.

[2] A. M. Binnie and S. G. Hooker, "The Flow Under Gravity of an Incompressible and Inviscid Fluid Through a Constriction in a Horizontal Channel, "Proceedings of the Royal Society, London," 159:592-608, 1937.

[3] Ernst Preiswerk, "Application of the Methods of Gas Dynamics to Water Flows with Free Surface."
Part 1. "Flows with no Energy Dissipation," NACA TM No. 934, 1940.
Part 2. "Flows with Momentum Discontinuities," NACA TM No. 935,1940.

[4] James Orlin, N. J. Linder and J. G. Bitterly, "Application of the Analogy Between Water Flow With a Free Surface and Two-Dimensional Compressible Gas Flow," NACA TN No. 1185, 1947.

[5] J. R. Bruman, "Application of the Water Channel Compressible Gas Analogy, "North American Aviation, Inc., Engineering Report NA-47-87, 1947.

analogy have been conducted at Massachusetts Institute of Technology by Harleman and Ippen.[6]

The initial work with the hydraulic analogy at the Daniel Guggenheim School of Aeronautics of the Georgia Institute of Technology was presented in a thesis by John Hatch[7] in 1949. He was responsible for the design and construction of the water channel and for conducting preliminary tests which demonstrated the possibilities that were presented in previous work. Additional tests, using improved methods for obtaining data were conducted by John Catchpole[8] in 1949 and Dallas Ryle[9] in 1950.

Points favoring the use of the hydraulic analogy as a tool for transonic and supersonic aerodynamic research may be summarized as follows:

(1) Initial cost and maintenance is very low as compared with wind-tunnel or free-flight tests, thus making it possible for small schools and colleges to have an inexpensive yet valuable instrument for high speed research and instruction.

---

[6] R. F. Harleman and A. T. Ippen, "Studies on the Validity of the Hydraulic Analogy to Supersonic Flow," U.S. Air Force Air Materiel Command Wright-Patterson Air Force Base, Dayton, Ohio, Technical Report No. 5985,1950.

[7] J. E. Hatch, "The Application of the Hydraulic Analogies to Problems of Two-Dimensional Compressible Gas Flow," Unpublished Master's thesis, Georgia Institute of Technology, Atlanta, 1949.

[8] E. J. Catchpole, "Application of the Hydraulic Analogy to Study the Performance of Two Airfoils in Compressible Flow." Unpublished Master's thesis, Georgia Institute of Technology, Atlanta, 1949.

[9] D. M. Ryle, Jr., "Application of the Hydraulic Analogy to Study the Performance of Three Airfoils at Subsonic and Supersonic Speeds." Unpublished Master's thesis, Georgia Institute of Technology, Atlanta, 1950.

(2) Various types of flow such as shock wave formation, vortices, and turbulence may be observed, measured and photographed with ease.

(3) Any given Mach number can be obtained by a simple adjustment of the speed of the motor.

(4) Visual observation of the flow in the transonic region is possible since the model passes through the sonic range at low speed.

The experiments performed in this thesis are concerned with the operation of a supersonic biplane. The scheme of using such a biplane to reduce the aerodynamic drag was first suggested by Busemann[10] at the Volta Conference in 1935.

The experiments described here were carried out with the two-fold purpose of comparing the existing theory and wind tunnel data by use of the hydraulic analogy, and also determining over what range the biplane was more efficient than a comparable single surface.

---

[10] A. Busemann, Atti del V Convegno "Volta", Rome, Reale Accademia d'Italia, 1935.

LIST OF SYMBOLS

a - Speed of sound in gas

C_D - Section drag coefficient

C_L - Section lift coefficient

C_p - Local pressure coefficient

c_p - Specific heat of gas at constant pressure

c_v - Specific heat of gas at constant volume

γ - Adiabatic gas constant, ratio of c_p to c_v

d - Water depth

$^\circ F$ - Degrees Fahrenheit

g - Acceleration of gravity

h - Enthalpy

M - Mach number

p - Pressure of gas

ρ - Density of gas

T - Absolute temperature of gas

V - Velocity of flow

ϕ - Velocity potential in two-dimensional flow

α - Angle of attack

x, y - Rectangular coordinates in the flow plane

u, v - Components of flow velocity in and directions, respectively

Subscripts

No subscripts - Any value of variable

l - Local value of variable

o - Value at stagnation

s - Value in undisturbed stream

max - Maximum value of variable

x - Partial derivative with respect to x

e.g. $\phi_x \equiv \frac{\partial \phi}{\partial x}$ $\phi_{xx} \equiv \frac{\partial^2 \phi}{\partial x^2}$

y - Partial derivative with respect to y

THEORY

Hydraulic Analogy

The theory of the analogy between water flow with a free surface and two-dimensional compressible gas flow is given in complete form by Preiswerk.[11] The pertinent points of the theory will be here summarized.

The following basic assumptions are made for this theory:

(1) The vertical acceleration of the water is negligible compared with the acceleration due to gravity. Hence, the pressure at any point in the fluid depends on the height of the free surface above the point in question.

(2) The flow is irrotational.

(3) There are no viscous or frictional losses, thus eliminating the conversion of energy into heat or external energy.

The fundamental relations for the analogy are obtained by setting up the energy equations for the two flows in terms of velocity. For water this equation gives

$$V^2 = 2g(d_o - d)$$

$$V_{max} = \sqrt{2 g d_o}$$

and for gas

$$V^2 = 2 g c_p (T_o - T)$$

$$V_{max} = \sqrt{2 g c_p T_o}$$

---

[11] Preiswerk. op. cit.

If the ratio of $\frac{V}{V_{max}}$ for the two flows are equated, the result is

$$\frac{d_o - d}{d_o} = \frac{T_o - T}{T_o} \quad OR$$

$$\frac{d}{d_o} = \frac{T}{T_o} \tag{1}$$

Thus, considering the velocity ratio the depth ratio is analagous to the temperature ratio of the gas.

A further condition for the analogy may be derived by comparison of the equations of continuity of the flows.

The continuity equation for water is

$$\frac{\partial (u d)}{\partial x} + \frac{\partial (v d)}{\partial y} = 0$$

and for two-dimensional gas flow

$$\frac{\partial (u \rho)}{\partial x} + \frac{\partial (v \rho)}{\partial y} = 0$$

From the above equation it can be seen that the water depth d is analagous to the gas density ρ, hence, a second condition for the analogy becomes

$$\frac{d}{d_o} = \frac{\rho}{\rho_o} \tag{2}$$

From a comparison of equations (1) and (2), the following relation is evident

$$\frac{T}{T_o} = \frac{\rho}{\rho_o} \tag{3}$$

The analogy will hold only so long as the above equation is satisfied by the gas in question. By assumption (3) it is known that the gas must also conform to the adiabatic relationship

$$\left(\frac{T}{T_o}\right)^{\frac{1}{\gamma-1}} = \frac{\rho}{\rho_o} \tag{4}$$

It is obvious upon inspection of equations (3) and (4) that for the analogy to hold, the gas in question must have $\gamma = 2$.

Thus, the above shows that for water flow to be analogous to that of a gas flow, the value of γ for the gas must equal 2. As the value of γ for air is 1.4 it would seem that use of the analogy may result in large errors in quantitative data. Such is not the case for a number of quantities do not vary greatly with a change in γ.

From the adiabatic relation and preceding relationships

$$\frac{p}{p_o} = \left(\frac{\rho}{\rho_o}\right)^{\gamma} = \left(\frac{\rho}{\rho_o}\right)^{2}$$

then

$$\frac{p}{p_o} = \left(\frac{d}{d_o}\right)^{2} \tag{5}$$

The differential equation for a two-dimensional water flow velocity potential is

$$\phi_{xx}\left(1-\frac{\phi_x^2}{gd}\right)+\phi_{yy}\left(1-\frac{\phi_y^2}{gd}\right)-2\phi_{xy}\left(\frac{\phi_x\,\phi_y}{gd}\right)=0 \tag{6}$$

and for a compressible gas

$$\phi_{xx}\left(1-\frac{\phi_x^2}{a^2}\right)+\phi_{yy}\left(1-\frac{\phi_y^2}{a^2}\right)-2\phi_{xy}\left(\frac{\phi_x\,\phi_y}{a^2}\right)=0 \tag{7}$$

The two above equations become analogous by placing $\frac{gd}{2gd_o} = \frac{a^2}{2gh_o}$.

As proven by Page[12], the velocity $\sqrt{gd}$ is the velocity of propagation of surface waves in shallow water when the wave length is great in comparison with the water depth and the surface tension is equal to zero.

Since the velocity of sound, a, is the velocity at which a small disturbance will be propagated in a gas flow, the Froude number $\frac{V}{\sqrt{gd}}$ for the shallow water flow is analogous to the Mach number in a gas flow.

When water is flowing at speeds above $\sqrt{gd}$, the flow velocity may decrease over a short distance resulting in an increase in depth. This type of unsteady motion is called a hydraulic jump, and corresponds to a shock wave in a gas.

The following table will summarize the corresponding analogous relations.

Two-Dimensional Compressible Gas Flow	Analogous Liquid Flow
Temperature ratio, $\frac{T}{T_o}$	Water-depth ratio, $\frac{d}{d_o}$
Density ratio, $\frac{\rho}{\rho_o}$	Water-depth ratio, $\frac{d}{d_o}$
Pressure ratio, $\frac{p}{p_o}$	Square of water-depth ratio, $\left(\frac{d}{d_o}\right)^2$
Velocity of sound, $a = \sqrt{\frac{\gamma p}{\rho}}$	Wave velocity, $\sqrt{gd}$
Mach number, $\frac{V}{a}$	Froude number, $\frac{V}{\sqrt{gd}}$
Shock wave	Hydraulic jump

[12] Leigh Page, Introduction to Theoretical Physics, New York, D. Van Nostrand Co. Inc., 1928, p. 218-224.

The application and corrections to the analogy as they will be used in this investigation follows:

The Mach number of the free stream may be calculated as

$$M_s = \frac{V_s}{\sqrt{g\, d_s}} \tag{8}$$

The equation for the pressure coefficient at any point on a surface is defined as

$$C_p = \frac{p_2 - p_s}{q_s} = \frac{p_2 - p_s}{\tfrac{1}{2} \rho_s V_s^2} \tag{9}$$

Now
$$\tfrac{1}{2} \rho_s V_s^2 = \tfrac{1}{2} \rho_s a_s^2 M_s^2$$
$$= \tfrac{1}{2} \rho_s \left(\frac{\gamma p_s}{\rho_s}\right) M_s^2$$
$$= \frac{\gamma}{2} p_s M_s^2$$

Giving for equation (9) upon simplifying

$$C_p = \frac{2}{\gamma M_s^2} \left[\left(\frac{p_2}{p_s}\right) - 1 \right]$$

using equation (5)
$$\frac{p_2}{p_s} = \frac{p_2}{p_o} \times \frac{p_o}{p_s} = \left(\frac{d_2}{d_o}\right)^2 \times \left(\frac{d_o}{d_s}\right)^2$$
$$= \left(\frac{d_2}{d_s}\right)^2$$

Therefore, taking $\gamma = 2$, the analogy gives the pressure coefficient as

$$C_p = \frac{1}{M_s^2} \left[\left(\frac{d_2}{d_s}\right)^2 - 1 \right] \tag{10}$$

The above equation may be corrected to $\gamma = 1.4$ by a method

proposed by Ryle[13] using figure 1 of NACA TN No. 1185.[14] The corrected equation is given as

$$C_p(\gamma=1.4) = \frac{1}{M_s^2}\left\{\left[\left(\frac{p_2}{p_o}\right)_{\gamma=1.4} \div \left(\frac{p_2}{p_o}\right)_{\gamma=2}\right]\left(\frac{d_2}{d_s}\right)^2 - 1\right\} \qquad (11)$$

Supersonic Biplane

The supersonic biplane was first conceived by Busemann.[15] A brief discussion of the biplane as a means of reducing drag at supersonic speeds will follow.

Theoretical and experimental results for supersonic profiles have shown that the drag of a profile increases approximately with the square of the maximum thickness. Therefore, the best profile for minimum drag or of maximum L/D is the flat plate. For structural reasons it would be impossible to use such a design in practice. The supersonic or Busemann biplane, as it is generally called, has theoretically the same wave or pressure drag as a flat plate at an equal angle of attack. However, it has a finite thickness making it a more practical design structurally.

---

[13] Ryle. op. cit.
[14] Orlin, Linder and Bitterly. op. cit.
[15] Busemann. op. cit.

The theoretical biplane is shown in Figure 1-A. The two profiles each have a leading and trailing edge with a zero deflection angle which gradually fairs into a flat surface. The front and rear surface for each profile intersects to form a vertex at the mid-chord. The profiles are placed vertically above each other in near proximity with the two flat base surfaces external and parallel. The flow that passes the biplane is divided into two parts: the flow that wets the external surfaces AB and CD, and the flow that goes into the channel AEBDFC. Since the leading edge of the profiles A and C are sharp, the phenomenon along AB and CD is the same as for the upper and lower surfaces of a flat plate of the same length and angle of attack. For the external part of the flow the biplane will be equivalent to the flat plate, as to wave drag, lift, and moment. Now, consider the internal flow. Along the profile portion AG and CH compression waves are generated. These compression waves are gradual due to the curved surface of the fore portion, and tend to form an envelope. Each of these envelopes cross each other and impinge on the central vertex of the opposite profile. The reflection of these waves may be avoided by having the wall of the profile aft of the central vertex in the same direction as the flow, thus, the compression wave will disappear. Therefore, the flow is compressed isentropically across two families of compression waves and disappears when meeting the opposite profile vertex. At the vertex of each profile the flow is then expanded isentropically with two families of expansion waves and attains again the conditions that the flow had before compression. This is

achieved by the cancellation of each expansion wave by the curved portion on the rear of each profile. Thus the resultant aerodynamic action of the internal flow is zero, and the biplane unit as a whole acts as a flat plate.

The experimental biplane used in the investigation differs in some respects from the ideal theoretical one. It is shown in Figure 1-B for the design condition and for the type of flow which exists with the experimental biplane. This biplane has a finite value for its leading and trailing edges instead of edges of zero angle as in the theoretical case. Since the edges are finite, a compression shock will occur on the leading edge of the profiles and the transformation in the internal flow will no longer be isentropic as the theory stated, but the differences are very small for small deflections. Also, a slight error is introduced by the trailing edge since the expansion waves are not completely cancelled out. This type of biplane presents a more practical design and the pressure drag is still very nearly that of a flat plate.

It should be stated that the Busemann biplane, though interesting from a theoretical standpoint, may be difficult to adapt to a practical aerodynamic design for the following reasons:

(1) It will operate ideally as a flat plate for only one angle of attack and for one Mach number.

(2) The drag due to friction will be greater since there are two profiles, therefore, part of the gain in pressure drag reduction is absorbed by the increased friction drag. At present it is not possible to evaluate just what skin friction drag amounts to unless the type of boundry layer is known.

EQUIPMENT

The water channel that was used for this investigation was of the type where the water remained at rest and the model moved. A general view of the channel is shown in Figure 2.

The water channel is four feet wide and twenty feet long, with a bolted structural steel framework. The channel bottom is fitted with one quarter-inch thick plate glass supported every thirty inches transversely. The glass was used to give a uniform surface for the model to slide on and for underwater lighting purposes. The channel legs are screw adjusted, so with the aid of a depth gage the water level at any point in the channel may be adjusted to ± .0001 if such accuracy is desired.

A drain was placed at one end of the channel bottom.

The movable model carriage is made of welded steel tubing to which an appropriate model mount is attached. The mount holds the model firmly to the channel bottom, allowing no water to flow beneath the model when in motion. The carriage moves along the channel rails on eight rubber wheels. Four of the wheels are mounted as to transfer the the weight of the carriage to the rails. The other four wheels are mounted one at each corner of the carriage with their axis of rotation vertical, thus eliminating any lateral movement of the carriage.

The carriage is driven by a one-quarter horse-power, single phase, alternating current electric motor using pulleys and a 3/22 inch continuous steel air craft cable. The carriage control is obtained

by a reversing mechanism and a "Speed-Ranger" device. This gives control of motion in either direction for low speeds. For high speed and accelerating runs an auxiliary power supply is used. The system consists of a 24 volt, 14.5 amp. direct current series wound motor, which drives the carriage cable through a set of reduction gears.

By use of the above arrangement steady speeds of from 0.5 to 5.5 feet per second may be realized with ease. A photograph of the drive mechanism is shown in Figure 3.

A means of accurately timing the speed of the model is made possible by use of a microswitch placed on the track. A cam 2.925 feet long is attached to the carriage and trips this switch which automatically operates a timer located on the control panel. The panel also contains switches for starting, reversing, operating the drive mechanism, and photo flood lights.

The first experimental data taken from the Georgia Tech water channel was the measure of the water depth distribution around a model by photographic means. The method and equipment used are given by Hatch[16]. Since this method did not give the desired accuracy, the probe method of measuring the water depth was developed.

When the probe method is used, the model is fitted with a plexiglass bracket mounted firmly on the top of the model. The probe is made by mounting a steel needle in a 1-1/2 inch bass screw. The screws are placed in brass bushings which are inserted in the plexiglass at the

---

[16] Hatch. op. cit.

points along the model profile that the water depth is to be measured and 0.1 inch off the model surface to avoid the meniscus of the model.

An aluminum contact was placed on each probe. The screw is adjusted until the probe touches the water. This completes the grid circuit of a vacuum tube, causing a relay to operate a signal light. The probes are adjusted from rear to front one at a time, until by use of the signal light the correct position of the probe is obtained. When all of the probes have been adjusted, the model is removed from the channel and the water depth at each local point on the model is measured by use of a height gage and surface plate to within an accuracy of 0.001 inch. A photograph of the biplane with probes in position moving down the channel is shown in Figure 4.

The Busemann biplane model was composed of two triangular G.U.4 airfoils, 6.1 per cent thick, 24 inch chord, and equal base angles of 7°. They were constructed of lacquered mahogany and were coupled by a fitting which allowed the gap between the profiles to be varied as desired. The model was designed to operate as a flat plate at a zero angle of attack and Mach number of 2.03. This resulted in a design gap of 10 inches. A drawing of the model will be found in Figure 5.

This particular configuration was investigated because an earlier supersonic wind tunnel program had been conducted by Ferri[17] on a similar model. The validity of the water channel data could thereby be readily compared with his results.

---

[17] A. Ferri, "Experiments at Supersonic Speed on a Biplane of the Busemann Type," R. T. P. Translation, No. 1407, 1940.

A single profile of the biplane was tested for comparison purposes and additional data for it is presented by Ferri[18], Catchpole[19], and Ryle[20].

---

[18] Ibid.

[19] Catchpole. op. cit.

[20] Ryle. op. cit.

PROCEDURE

Preceding each test run, the static water depth of the test area of the channel was adjusted to a depth of .25 inch. The carriage speed was then adjusted until the timer read the correct calculated time for the Mach number desired. The probes were adjusted and the resulting depths measured as described in the previous section.

The angle of attack of the model was set by positioning the leading and trailing edges relative to the channel sides by means of a steel rule.

TESTS CONDUCTED

For all tests a Mach number of 2.03 was used with a static water depth of .25 inch. The conditions tested were as follows:

Busemann Biplane

Gap ratio	.8	0, 2, 4, 6 degrees
Gap ratio	1.0	0, 2, 4, 6 degrees
Gap ratio	1.3	0, 2, 4, 6 degrees
Gap ratio	1.6	0, 2, 4, 6 degrees
Gap ratio	1.8	0, 2, 4, 6 degrees

Single Biplane Profile

0, 2, 4, 6 degrees

COMPARISON AND DISCUSSION

Visual Observations

Presented in Figures 6, 7, 8, and 9 are examples of the typical flow patterns that were encountered during the experiments.

Figure 6 shows the biplane moving down the channel under the design conditions $\alpha = 0^{\circ}$, gap ratio = 1, and $M = 2.03$. The measurement of the shock angles from the photograph gave excellent results when compared with "exact" shock theory as found in Bonney[21], for this condition varying less than .2 of a degree. It is noted that weak shocks are present on both external surfaces which are not predicted by theory. Their presence explains the existence of positive pressure coefficients for these surfaces which appear on the pressure distribution curves in Figure 10. The shock waves also occur in wind tunnel tests, as shown by Ferri[22] for a similar model.

Figure 7 presents the same conditions as Figure 6, except $\alpha = 6^{\circ}$. The change in flow pattern is readily observed by comparing the two figures. Again there is very close agreement between the measured shock angle and the theoretical one.

Figures 8 and 9 are examples of the flow pattern for other than the design gap ratio. Their gap ratio is equal to 1.6 of the design gap.

---

[21] E. A. Bonney, Engineering Supersonic Aerodynamics. New York, McGraw-Hill Book Co. Inc., 1950, pp. 79-104.

[22] Ferri. op. cit.

Figure 8 is for $\alpha = 0^{\circ}$ and it is observed that after the shock wave intersection the waves assume a slightly curved path. This is caused by the intersection of each shock wave with the expansion region which is produced at the central vertexes. The small waves parallel to the surfaces and behind the shock waves have no bearing on the flow pattern as they were caused by a momentary vibration of the model.

Figure 9 is the flow condition for $\alpha = 6^{\circ}$. The weak shock wave produced at the leading edge of the upper surface on the lower profile was almost eliminated by the strong shock from the leading edge of the upper profile. For the condition of large gap ratios the shock wave angle was in greater error, as may be expected. However, the difference between theory and measurement was never over 2°.

Pressure Coefficients and Lift and Drag Coefficients

Representative chordwise and thickness pressure distribution curves are contained in Figures 10 through 17. The data was obtained as described in the previous section. The pressure coefficients were corrected to a $\gamma = 1.4$ by use of Equation 11. A sample of the method of calculation is given in Table I of Appendix I.

Figures 10 and 12 represent the change in chordwise pressure distribution with angle of attack for the design gap ratio. Figure 11 contains the thickness pressure distribution for the design gap at $\alpha = 0^{\circ}$.

Figures 13 and 14 show the type of chordwise pressure distribu-

tion for a single profile of the biplane at $\alpha = 0$. Similar curves for this model at different angles of attack and Mach number are presented by Catchpole[23] and Ryle.[24]

Figure 17 gives a typical thickness pressure distribution for the single profile and when compared with Figure 11 indicates the large drag reduction possible for equal angles of attack.

By mechanical integration of the chordwise and thickness pressure distributions the lift and drag coefficients for the biplane and single profile were obtained. These are plotted in Figures 18 and 19 along with the "exact" theory and the experimental results of Ferri[25]. A tabulation of all the lift and drag coefficients for the conditions tested will be found in Appendix I, Tables II and III.

Figure 18 presents the lift and drag coefficient curves for the biplane at the design gap. The drag test points follow the theoretical curve at low angles of attack and approach the wind tunnel curve at the larger angles. The same trend is observed for the lift coefficient also.

The lift and drag coefficient curves for the single profile are given in Figure 19. The test points show the same trends as are found in the biplane with the exception that the lift does not approach the wind tunnel results as closely as in the biplane. The lift for $\alpha = 0$ appears to be in large error, compared with theory. This deviation is

---

[23] Catchpole. op. cit.

[24] Ryle. op. cit.

[25] Ferri. op. cit.

caused, as can be seen in Figure 16, by the small absolute pressure coefficient which theory predicted and was not realized in the water channel measurements. The fault for this condition is not in the hydraulic analogy, but in the inability to make proper correction to the pressure coefficients along the model surface due to the friction of the water on the surface.

The presentation of Figures 20 and 21 will indicate the trends of the lift and drag coefficients as a function of the biplane gap ratio for each angle of attack tested.

Figure 20 contains the lift data for all points tested. The water channel data definitely follows the trends of the theory and wind tunnel results. The test points follow the wind tunnel results somewhat more closely than theory, with the greatest deviation occuring at the large gap ratios and angles of attack. For the $\alpha = 0$ condition, the lift in each case was very small.

Figure 21 indicates an increase in drag coefficient with both angle of attack and gap ratio. The test points coincide more closely with theory for the small angles of attack and large gap ratios. The largest error with wind tunnel results appears for an angle of attack of 0^{o}.

As stated under Tests Conducted, data was to have been taken at a gap ratio $= 0.8$. When the tests were carried out it was found impossible to decrease the bap below the design gap and still maintain the flow conditions desired. A normal shock wave formed at the biplane

minimum section and moved toward the leading edge. A phenomenon of this type was found by Ferri[26] to exist in the wind tunnel under certain conditions.

Evaluation of Biplane

By the use of Figures 22 through 23 an endeavor will be made to evaluate over what range of gap ratio and angle of attack the biplane tested will be a superior and more efficient arrangement when compared with a single biplane profile.

As mentioned previously, the biplane will have a larger value for its skin friction than will the single profile. The drag coefficients presented do not include a value for the skin friction. Therefore, the drag of the biplane should be increased in some manner to make the comparison of a closer quantitative value. At present no means is known to make this correction, however, some method may possibly be developed employing local velocity, surface finish of the model, and friction of the water on the model to obtain a value for the frictional drag. For the following comparison the drag as presented will be used.

When the lift-drag ratio is plotted as a function of the gap ratio for each angle of attack as in Figure 22, definite trends make their appearance. The lift-drag ratio decreases with increasing gap ratio and increases in diminishing increments for an increase in

---

[26] Ferri. op. cit.

angle of attack. For an $\alpha = 6^{\circ}$ the lift-drag ratio is less than that for $\alpha = 4^{\circ}$ in the small gap ratio range, and only slightly greater than 4° in the large gap ratio range. It is concluded from the above that there is nothing to be gained by operating this biplane configuration above an angle of attack of 6°.

Figure 23 approximately indicates over what range of gap ratio and angle of attack that the biplane lift-drag ratio exceeds that of a single profile. The figure indicates that the biplane may have a gap ratio slightly in excess of 1.3 and operate at an angle of attack up to approximately 6° and still possess a larger lift-drag ratio than that of the single profile.

In order to make the results of a more practical value, Figure 24 was included. The curve was set up in the following manner. The biplane designed for ideal operation at $M = 2.03$, $\alpha = 0^{\circ}$, and gap ratio $= 1.0$ was taken as a reference model. Then by use of the shock charts presented in Bonney[27], ideal theoretical Mach numbers for number of similar biplanes to give minimum drag were calculated for different gaps. Thus, the resulting curve represents the ideal Mach number of the biplane investigated for various gap ratios. This is given in Figure 24 along with the test points of the investigation.

Although the biplane may be operated with considerable efficiency at other than the design condition, the most practical solution for a large speed variation is deduced from Figure 24. If the wings were con-

---

[27] Bonney. op. cit.

structed in such a manner that the gap ratio could change in flight in accordance with the theoretical curve, the high lift-drag ratio could be retained and the only loss would be due to angle of attack variation.

General Discussion

The results of the lift and drag coefficients were of an acceptable accuracy when compared with theory and wind tunnel values. Generall, the results were not as close those presented by Ryle[28]. This was to be expected because of the inability to hold the static water depth of the channel constant over the large area covered by the biplane model. This was a particular problem for the large gap ratios. This condition definitely introduced an error which was not encountered in previous work.

The use of a large scale model may in some respect compensate for the above error. A Reynolds number of 387,000 was obtained at a water temperature of 86°F. for this model. Ryle[29] showed that a Reynolds number of this magnitude produced more accurate results than that of smaller scale, lower Reynolds number models. Ferri's[30] wind tunnel tests were conducted at a Reynolds number of 600,000.

---

[28] Ryle. op. cit.

[29] Ibid.

[30] Ferri. op. cit.

As both the hydraulic analogy and theory do not consider viscous losses, it would seem that the water channel data would compare more closely with that of theory than wind tunnel data.

CONCLUSIONS

The following conclusions are made on the basis of the results of the investigation:

(1) That the hydraulic analogy presents a convenient, inexpensive, and reliable means of studying supersonic shock and expansion wave interaction and also supplies quantitative results of an acceptable value.

(2) That the supersonic biplane may lead to notable advantages both from the point of view of the reduction of drag, and of the increase in the efficiency of the wing unit.

(3) That the biplane may be operated at gap ratios up to 1.3 and at angles of attack up to 6° for a design Mach number and still maintain a lift-drag ratio in excess of a single profile.

RECOMMENDATIONS

It is recommended that a further study be made into the phenomenon of the normal shock wave formation for gap ratios less than unity. Also of value would be an investigation of a biplane model designed to operate under ideal conditions at an angle of attack and tested at various Mach numbers instead of gap ratios.

BIBLIOGRAPHY

A. Fundamental Theory

Bonney, E. Arthur, Engineering Supersonic Aerodynamics. New York, McGraw-Hill Book Co., 1950. 264 pp.

Courant, Richard, and K. O. Friedrichs, Supersonic Flow and Shock Waves. New York, Interscience Publishers, Inc., 1948. 464 pp.

Ferri, Antonio, Elements of Aerodynamics of Supersonic Flows. New York, The Macmillan Company, 1949. 434 pp.

Hunsaker, Jerome Clarke, and B. G. Rightmire, Engineering Applications of Fluid Mechanics. New York, McGraw-Hill Book Co., 1947. 494 pp.

Lamb, Horace, Hydrodynamics. Sixth Edition. London, Cambridge University Press, 1932. 737 pp.

Liepmann, Hans Wolfgang, and Allen E. Puckett, Introduction to Aerodynamics of a Compressible Fluid. New York, John Wiley and Sons, Inc., 1947. 262 pp.

Rouse, Hunter, Elementary Mechanics of Fluids. New York, John Wiley & Sons, Inc., 1946. 376 pp.

Sibert, Harold Ward, High-Speed Aerodynamics. New York, Prentice-Hall, Inc., 1948. 289 pp.

Streeter, Victor Lyle, Fluid Dynamics. New York, McGraw-Hill Book Co., 1948. 263 pp.

B. The Hydraulic Analogy

Binnie, A. M. and S. H. Hooker, "The Flow Under Gravity of an Incompressible and Inviscid Fluid Through a Constriction in a Horizontal Channel," Proceedings of the Royal Society, London, 159: 592-608, 1937.

Bruman, J. R., "Application of the Water Channel-Compressible Gas Analogy," North American Aviation, Inc., Engineering Report, No. NA 47-87, 1947. 60 pp.

Catchpole, Eric John, The Application of the Hydraulic Analogy to Study the Performance of two Airfoils in Compressible Flow. Unpublished Master's thesis, Georgia Institute of Technology, Atlanta, 1949. 62 pp.

Harleman, R. F. and Arthur T. Ippen, "Studies on the Validity of the Hydraulic Analogy to Supersonic Flow," United States Air Force Air Materiel Command Wright-Patterson Air Force Base, Dayton, Ohio, Technical Report No. 5985, Parts I and II, 1950. 130 pp.

Hatch, John Elmer, Jr., The Application of the Hydraulic Analogies to Problems of Two-Dimensional Compressible Gas Flows. Unpublished Master's thesis, Georgia Institute of Technology, Atlanta, 1949. 57 pp.

Orlin, W. James, Norman J. Linder, and Jack G. Bitterly, "Application of the Analogy Between Water Flow with a Free Surface and Two-Dimensional Compressible Gas Flow," U. S. National Advisory Committee for Aeronautics Technical Note No. 1185, 1947. 20 pp.

Preiswerk, Ernst, "Application of the Methods of Gas Dynamics to Water Flows with Free Surface."
Part I. "Flows with no Energy Dissipation," U. S. National Advisory Committee for Aeronautics Technical Memorandum No. 934, 1940. 60 pp.
Part II. "Flows with Momentum Discontinuities (Hydraulic Jumps)." U. S. National Advisory Committee for Aeronautics Technical Memorandum No. 935, 1940. 56 pp.

Riabouchinsky, D., "Mecanique des Fluides-Sur l'Analogie Hydraulique des Movements d'un Fluide Compressible," Comptes Rendus 195:No.22: 998-999, 1932.

Ryle, Dallas Marlin, Jr., Application of the Hydraulic Analogy to Study the Performance of Three Airfoils at Subsonic and Supersonic Speeds. Unpublished Master's thesis, Georgia Institute of Technology, Atlanta, 1950. 77 pp.

Thomas, Gerald B., "Application of Water Channel-Compressible Gas Analogies to Problems of Supersonic Wind Tunnel Design. Unpublished Master's thesis, Georgia Institute of Technology, Atlanta, 1949. 55 pp.

C. Wind Tunnel Test Results

Ferri, Antonio, "Completed Tabulation in the United States of Tests of 24 Airfoils at High Mach Numbers," U. S. National Advisory Committee for Aeronautics Wartime Report No. L-143. 21 pp.

———, "Experiments at Supersonic Speed on a Biplane of the Busemann Type," R. T. P. Translation No. 1407, 1940. 45 pp.

D. Other References

Busemann, A., Atti del V Convegno "Volta," Rome, Reale Accademia d'Italia, 1935.

Lighthill, M. J., "A Note on Supersonic Biplanes," British Aeronautical Research Council Reports and Memoranda No. 2002, 1944. 5 pp.

Page, Leigh, Introduction to Theoretical Physics. New York, D. Van Nostrand Co. Inc., 1928. 482 pp.

APPENDIX I

TABLES

TABLE I

SAMPLE CALCULATION OF PRESSURE COEFFICIENT FROM EXPERIMENTAL DATA

Single profile of the biplane, $\alpha = 0°$, $d_s = 0.25$ inch, $d_o = 0.766$ inch[31]

Timer reading = 1.76 seconds, Timer cam length = 2.925 feet

$$\therefore M_s = \frac{V_s}{\sqrt{gd}} = \frac{\frac{2.925}{1.76}}{\sqrt{g \times \frac{.250}{12}}} = 2.03, \frac{1}{M_s^2} = .243$$

$$C_p(\gamma=1.4) = \frac{1}{M_s^2}\left\{\left[\left(\frac{P_2}{P_o}\right)_{\gamma=1.4} \div \left(\frac{P_2}{P_o}\right)_{\gamma=2}\right]\left(\frac{d_2}{d_s}\right)^2 - 1\right\}$$

(1) Station (chord)	(2) d_1/d_s	(3) d_1/d_o	(4) (p_1/p_o) =1.4	(5) (p_1/p_o) =2.0	(6) (4)/(5)	(7) $(d_1/d_s)^2$	(8) (6)x(7)	C_p (=1.4)
Lower surface								
25.00	1.023	.334	.127	.109	1.16	1.046	1.210	.051
75.00	1.031	.337	.130	.115	1.13	1.078	1.218	.053
Upper surface								
16.67	1.200	.391	.175	.146	1.20	1.440	1.722	.175
33.33	1.183	.386	.170	.145	1.17	1.400	1.638	.155
66.67	1.208	.394	.176	.147	1.20	1.460	1.745	.181
83.33	1.191	.389	.173	.145	1.18	1.420	1.670	.163

[31] Orlin, Linder and Bitterly. op cit., Eqn. 12a

TABLE II

EXPERIMENTAL VALUES OF LIFT AND DRAG

COEFFICIENTS FOR THE BUSEMANN BIPLANE

M = 2.03, Gap ratio = 1.0

α (degrees)	C_L	C_D
0	.0052	.00254
2	.131	.0158
4	.196	.0255
6	.328	.0542

M = 2.03, Gap ratio = 1.3

α (degrees)	C_L	C_D
0	.0124	.0139
2	.105	.0267
4	.221	.0372
6	.352	.0586

M = 2.03, Gap ratio = 1.6

α (degrees)	C_L	C_D
0	.0110	.0240
2	.141	.0438
4	.272	.0515
6	.420	.0710

M = 2.03, Gap ratio = 1.8

α (degrees)	C_L	C_D
0	.0165	.0351
2	.153	.0470
4	.287	.0605
6	.437	.0827

TABLE III

EXPERIMENTAL VALUES OF LIFT AND DRAG COEFFICIENTS

FOR SINGLE PROFILE OF THE BUSEMANN BIPLANE

M = 2.03

α (degrees)	C_L	C_D
0	.0116	.0154
2	.0652	.0189
4	.123	.0217
6	.203	.0337

APPENDIX II

FIGURES

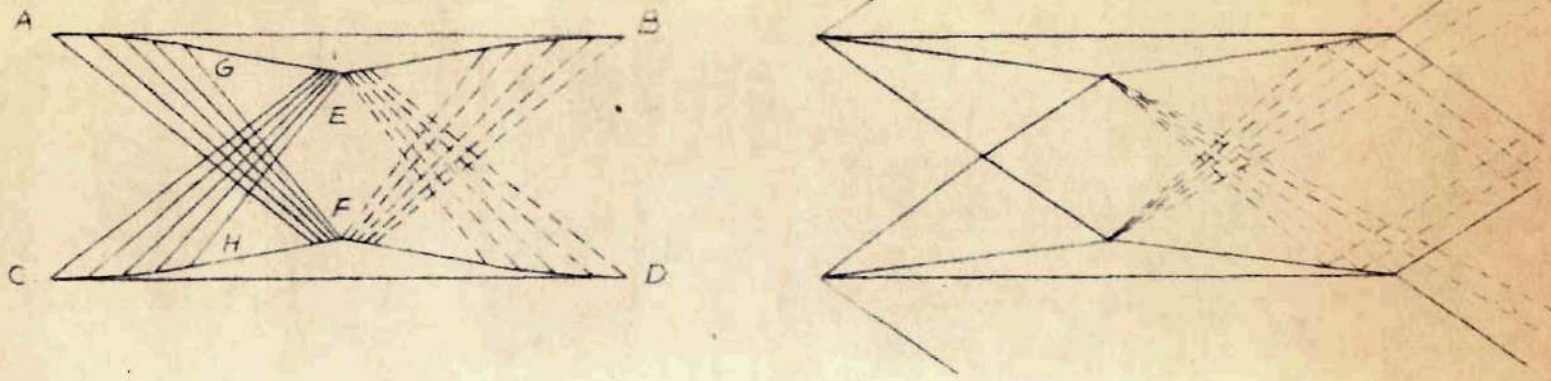

THEORETICAL BIPLANE
A

EXPERIMENTAL BIPLANE
B

FIGURE 1.- COMPARISON OF THEORETICAL AND EXPERIMENTAL BIPLANES

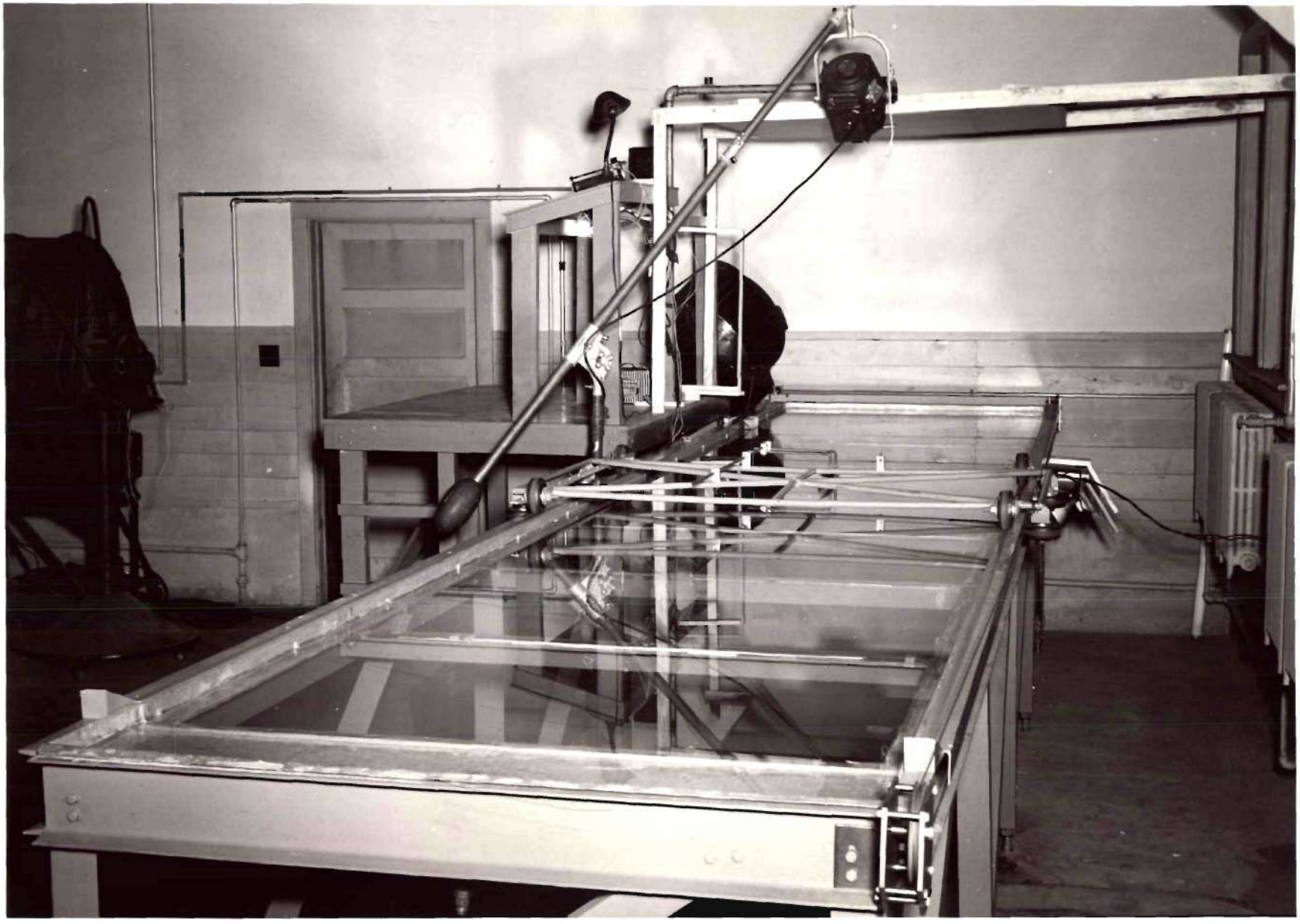

FIGURE 2
GENERAL VIEW OF WATER CHANNEL

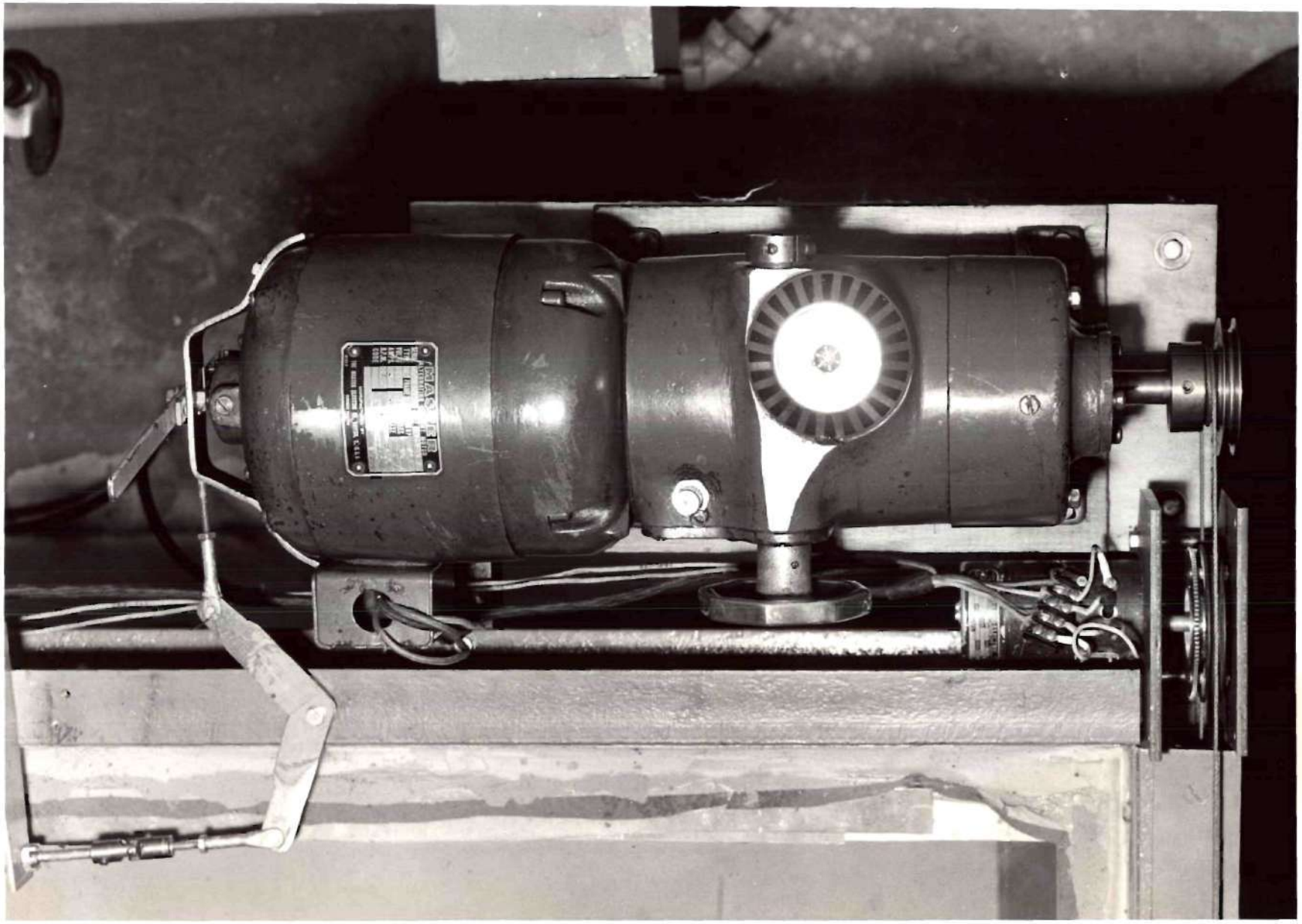

FIGURE 3

CARRIAGE DRIVE MECHANISM

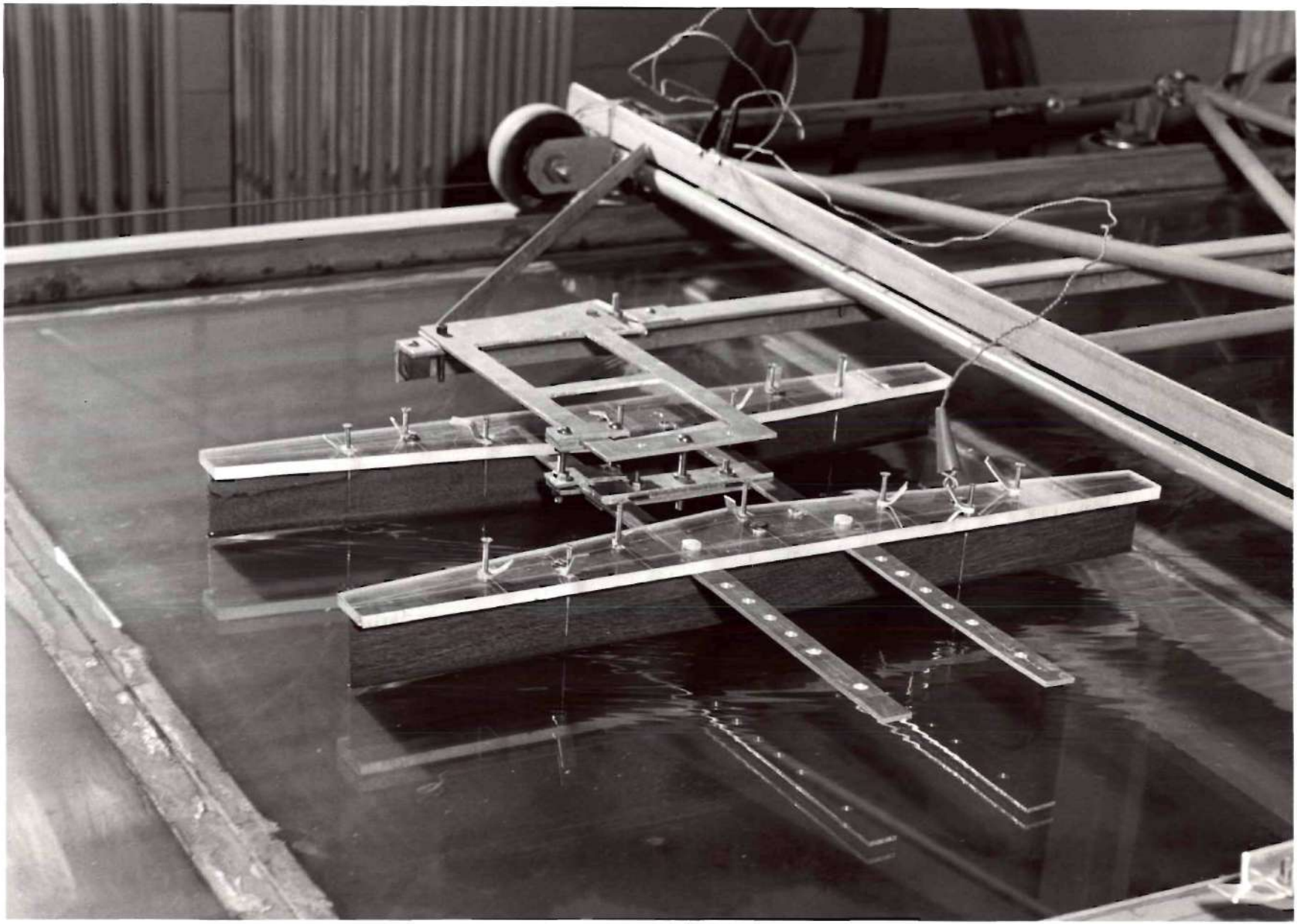

FIGURE 4
MODEL UNDER TEST CONDITIONS

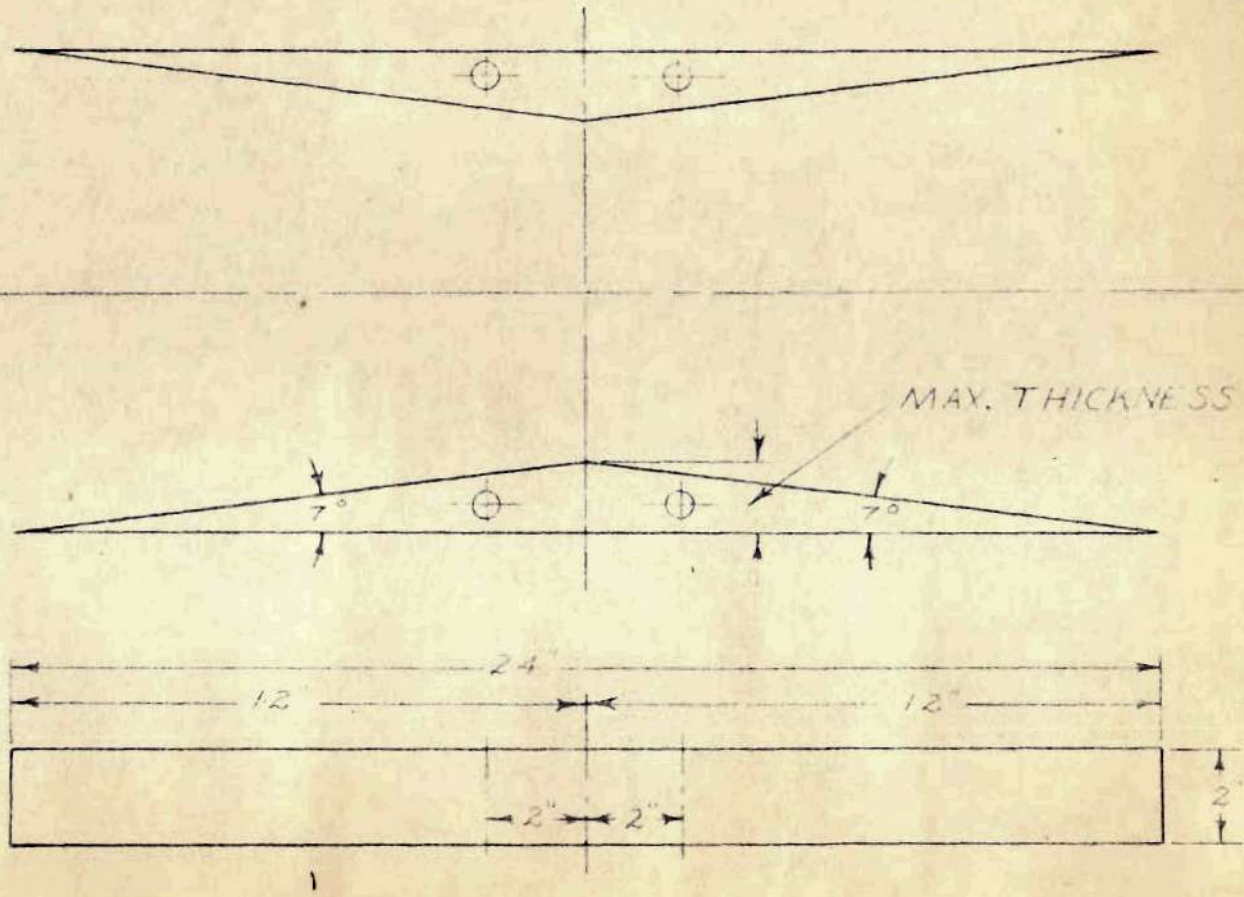

FIGURE 5. - BIPLANE MODEL

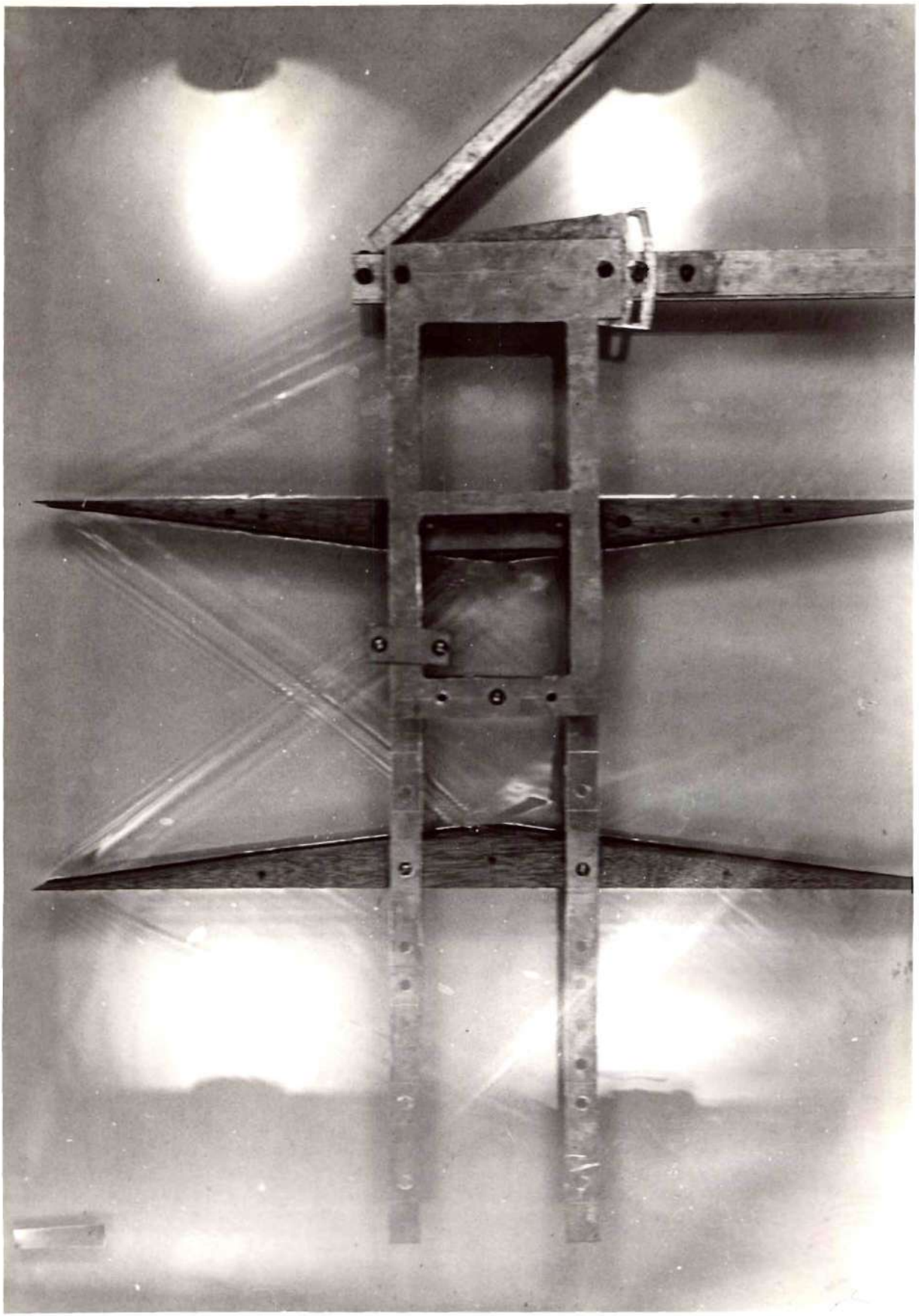

FIGURE 6

FLOW ABOUT MODEL FOR M = 2.03, $\alpha = 0^{\circ}$, GAP RATIO = 1.0

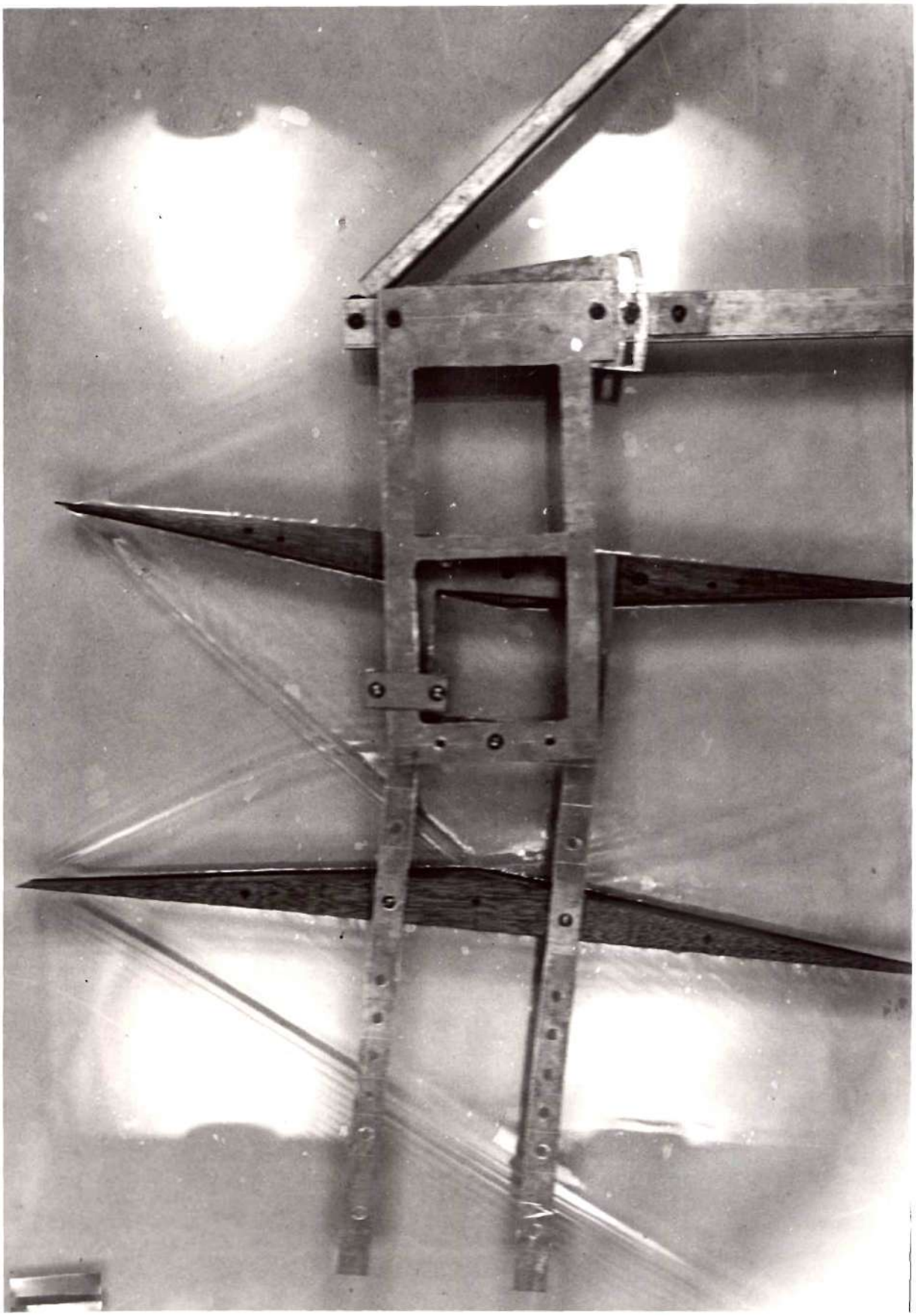

FIGURE 7

FLOW ABOUT MODEL FOR M = 2.03, α = 6°, GAP RATIO = 1.0

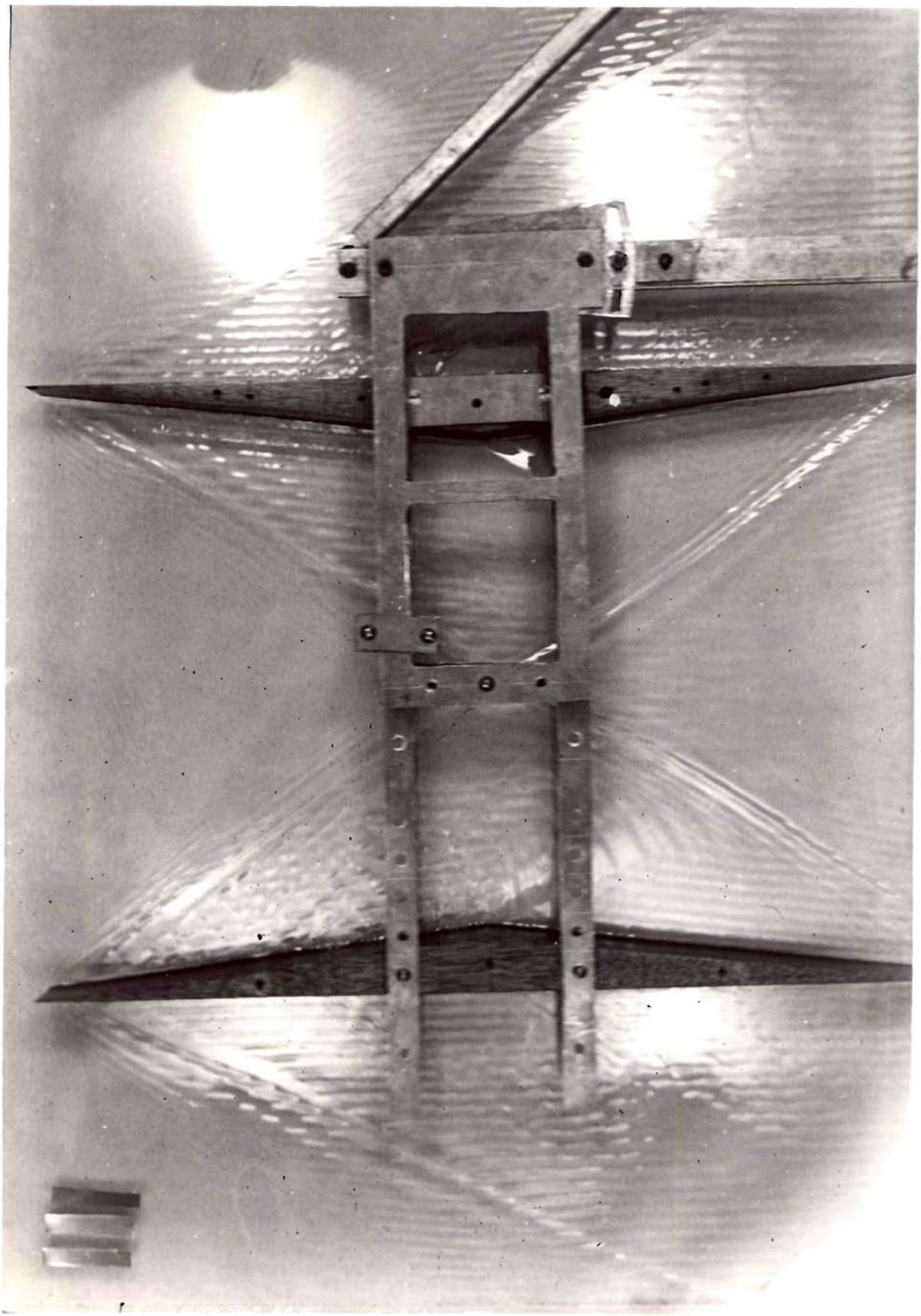

FIGURE 8

FLOW ABOUT MODEL FOR M = 2.03, α = 0^{0}, GAP RATIO = 1.6

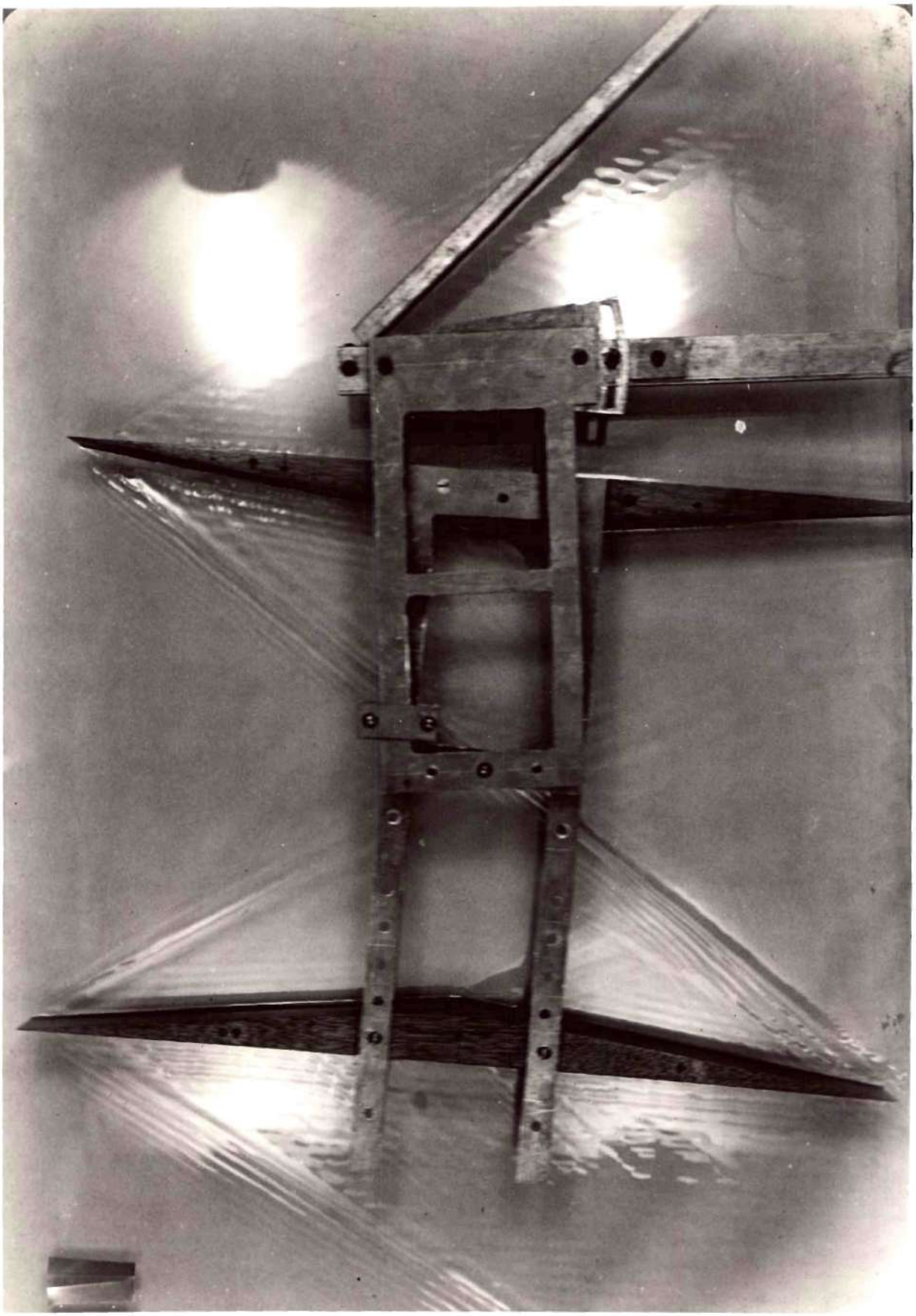

FIGURE 9

FLOW ABOUT MODEL FOR M = 2.03, $\alpha = 6^{\circ}$, GAP RATIO = 1.6

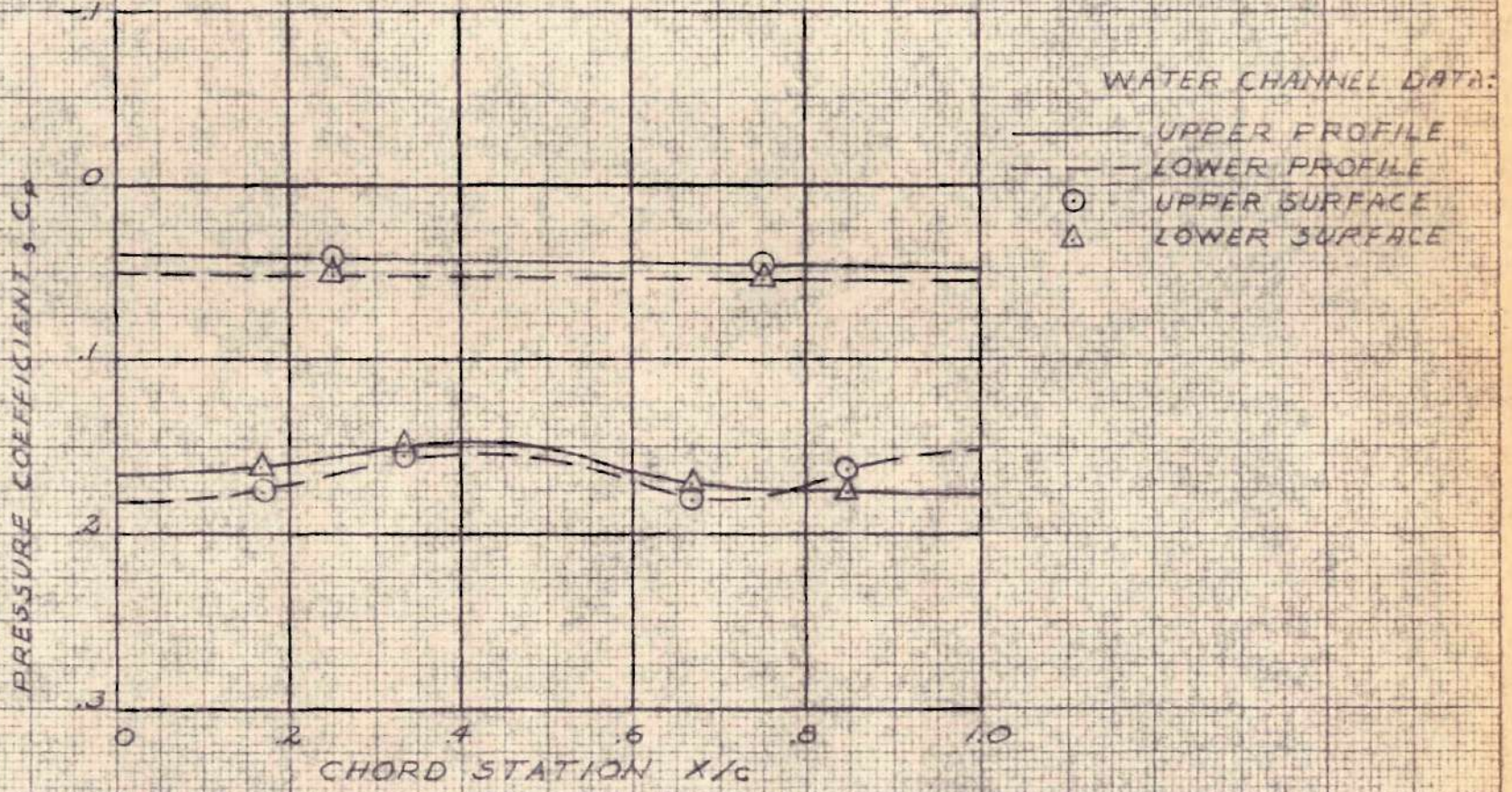

FIGURE 10. - CHORDWISE PRESSURE DISTRIBUTION FOR BIPLANE AT $M = 2.03$, $\alpha = 0°$, GAP RATIO = 1.0

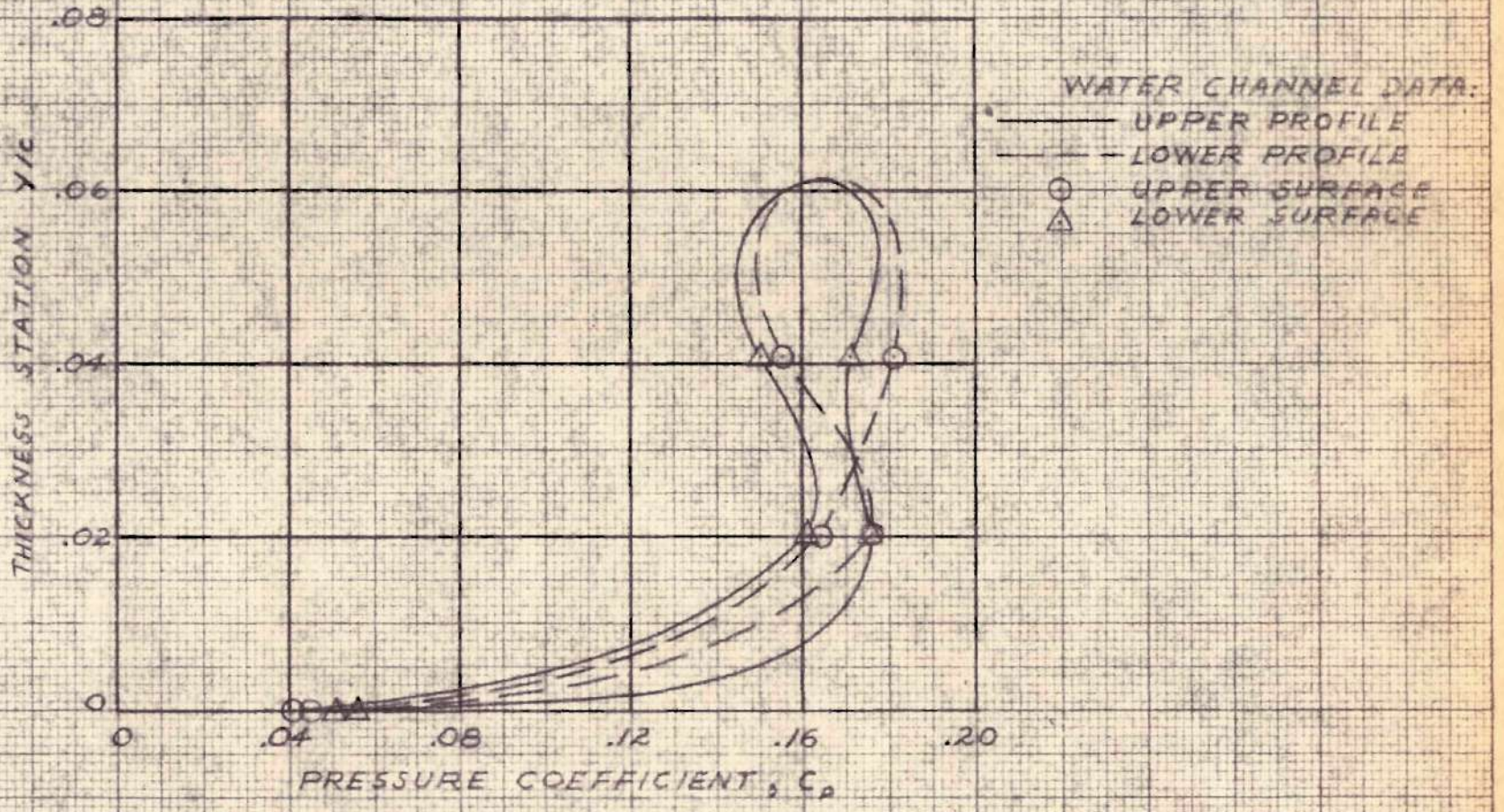

FIGURE 11.- THICKNESS PRESSURE DISTRIBUTION FOR BIPLANE AT M= 2.03, $\alpha = 0°$, GAP RATIO = 1.0

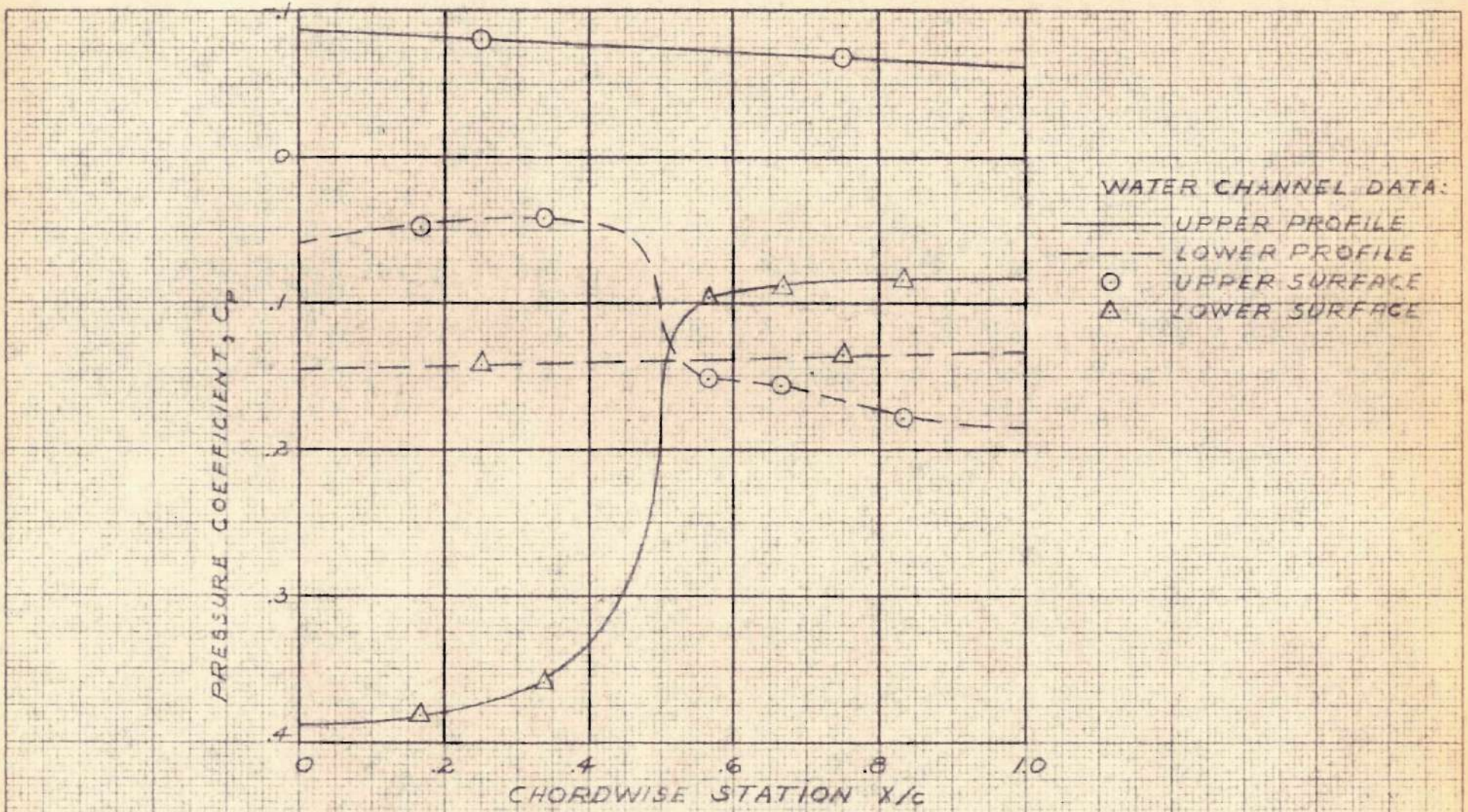

FIGURE 12.- CHORDWISE PRESSURE DISTRIBUTION FOR BIPLANE AT $M = 2.03$, $\alpha = 6°$, GAP RATIO = 1.0

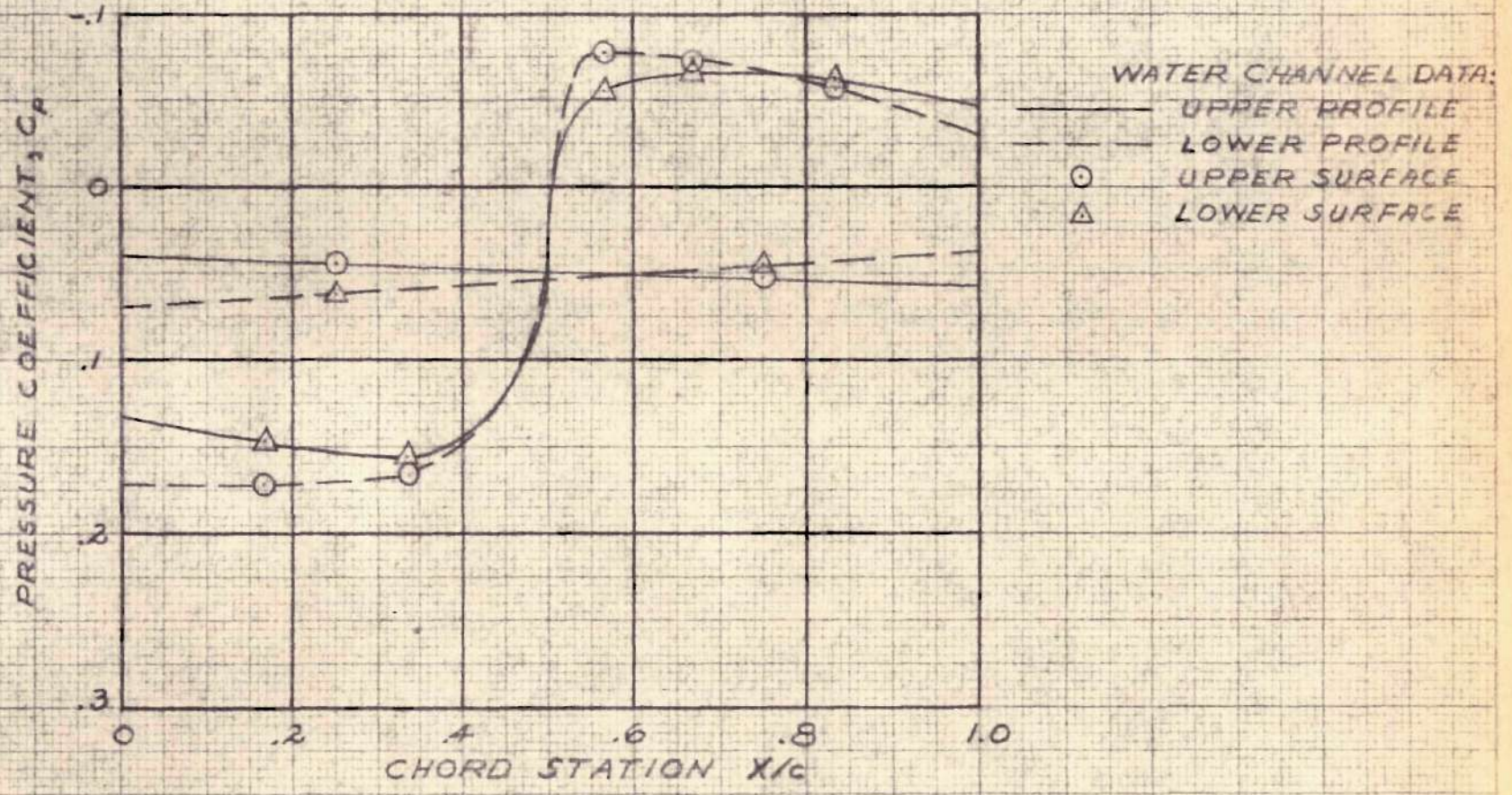

FIGURE 13.- CHORDWISE PRESSURE DISTRIBUTION FOR BIPLANE AT $M = 2.03$, $\alpha = 0°$, GAP RATIO = 1.6

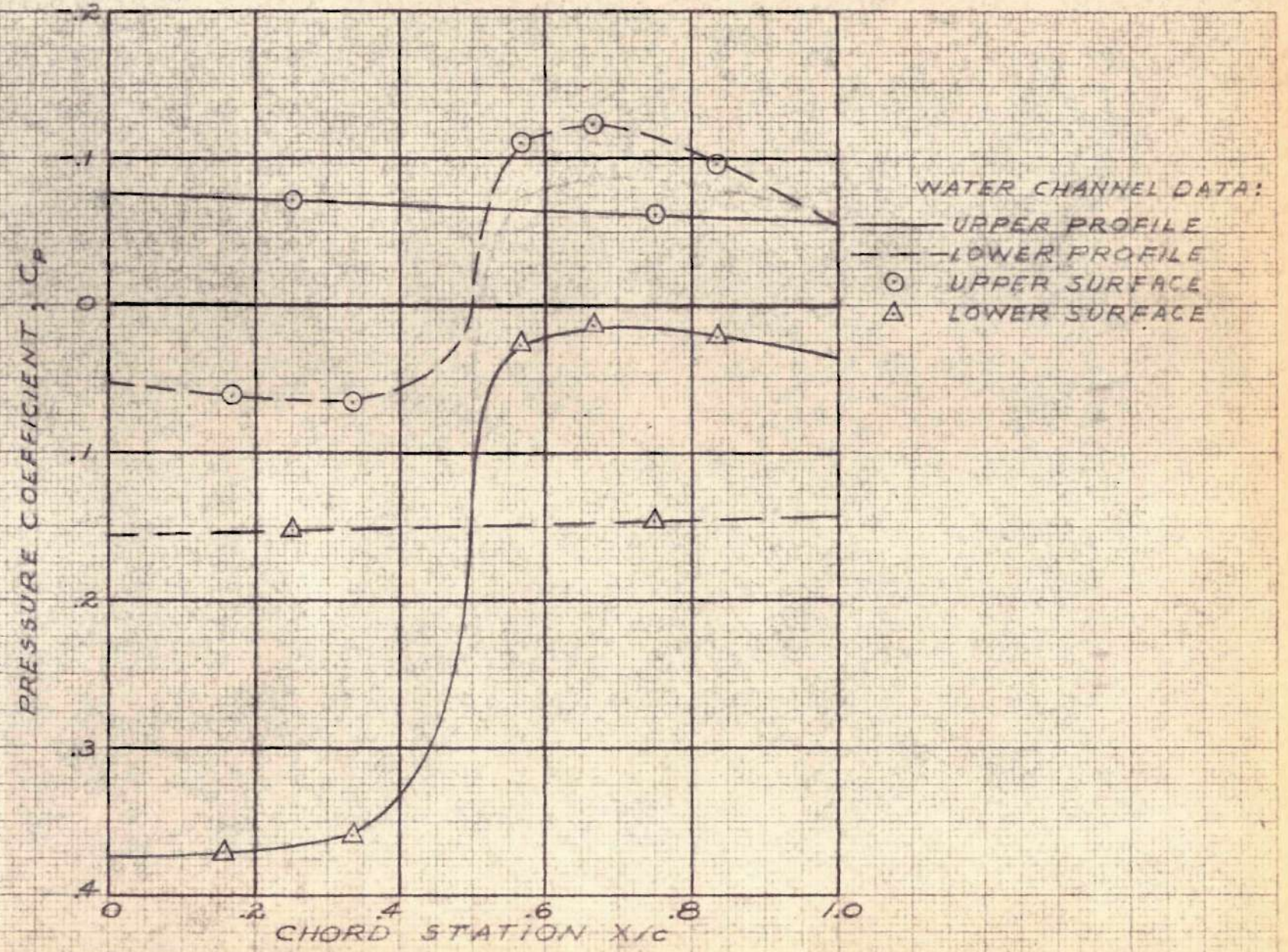

FIGURE 14. - CHORDWISE PRESSURE DISTRIBUTION FOR BIPLANE AT $M = 2.03$, $\alpha = 6°$, GAP RATIO = 1.6

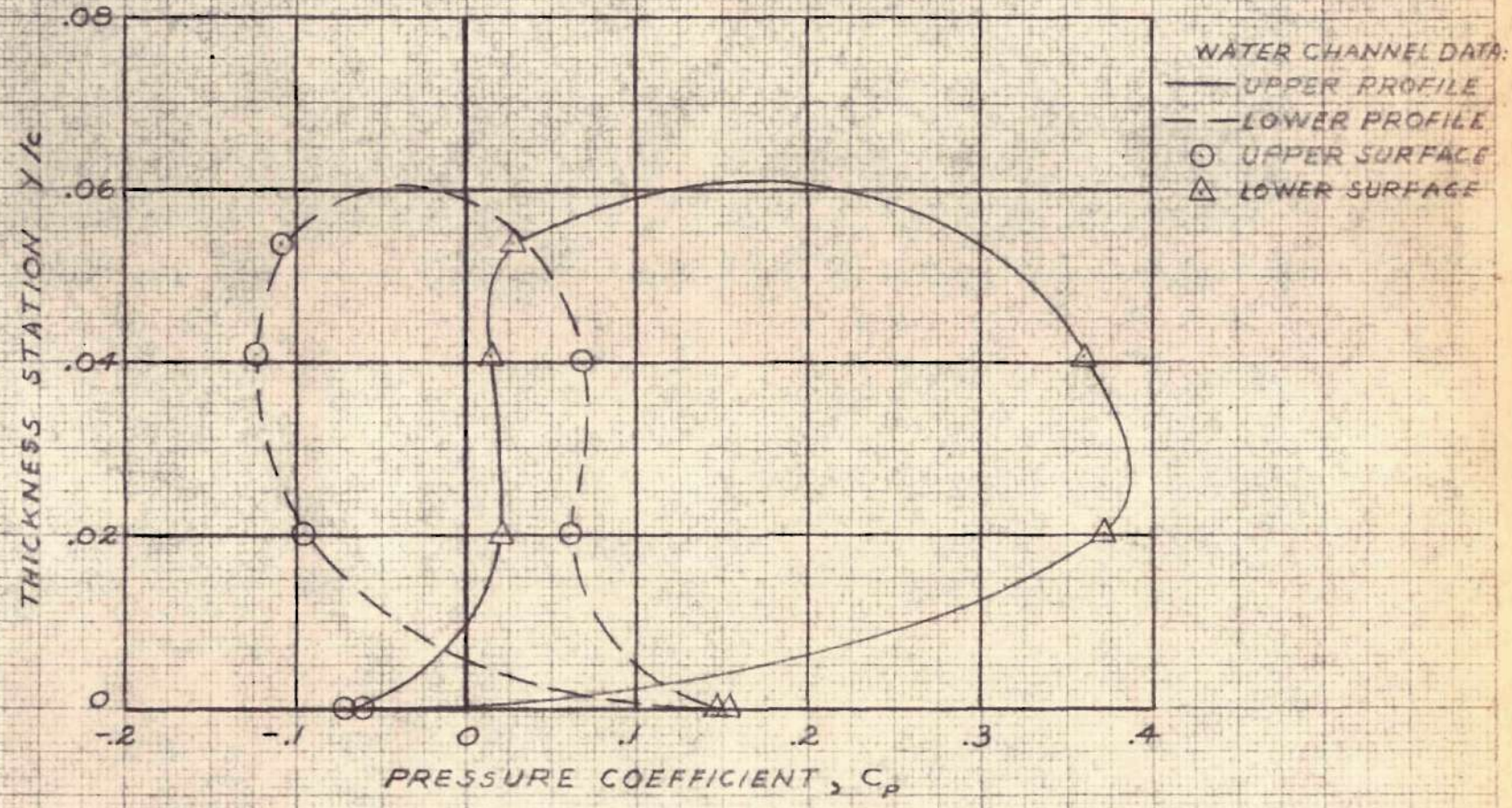

FIGURE 15.- THICKNESS PRESSURE DISTRIBUTION FOR BIPLANE AT $M = 2.03$, $\alpha = 6°$, GAP RATIO = 1.6

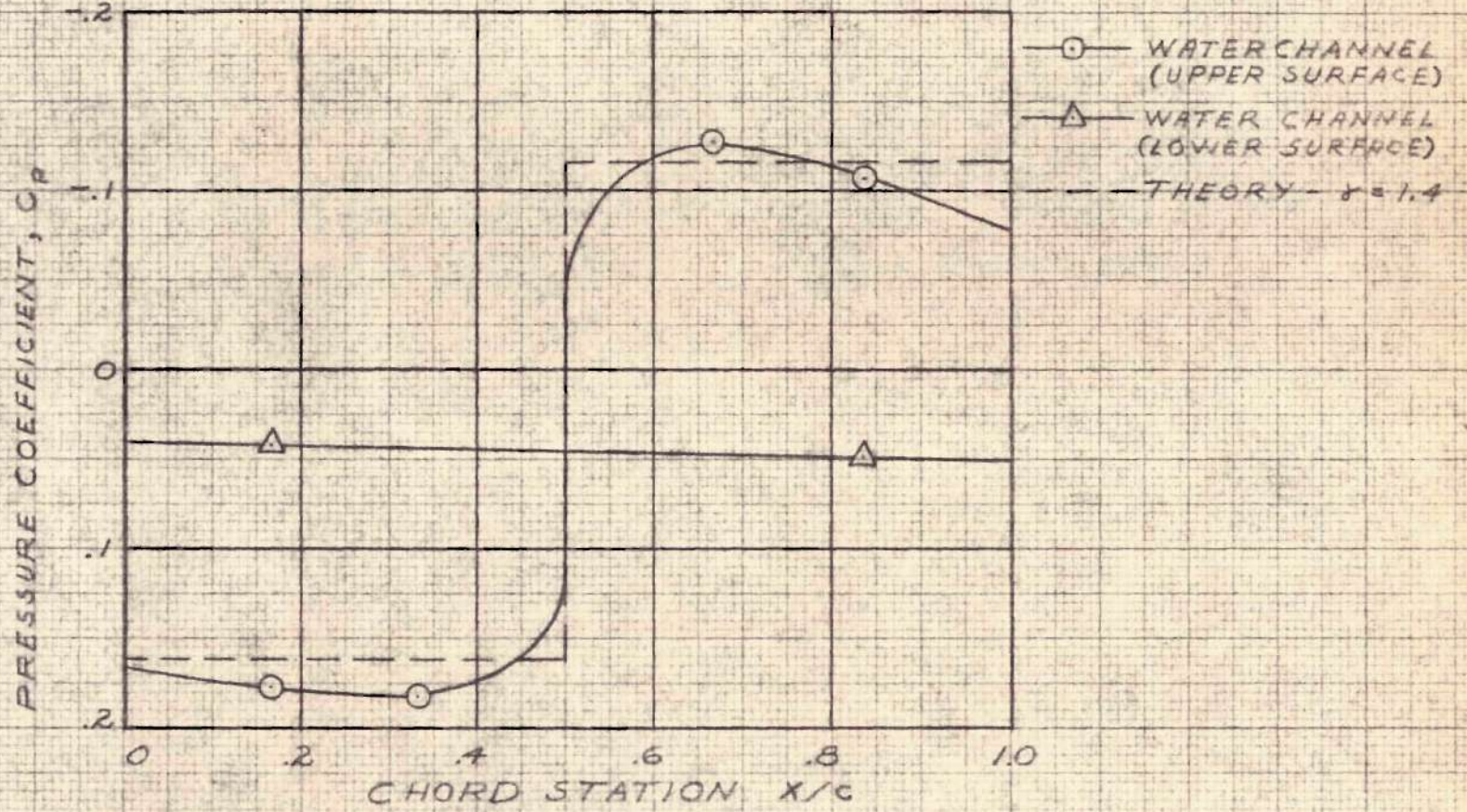

FIGURE 16. - CHORDWISE PRESSURE DISTRIBUTION FOR SINGLE BIPLANE PROFILE AT $M = 2.03$, $\alpha = 0°$

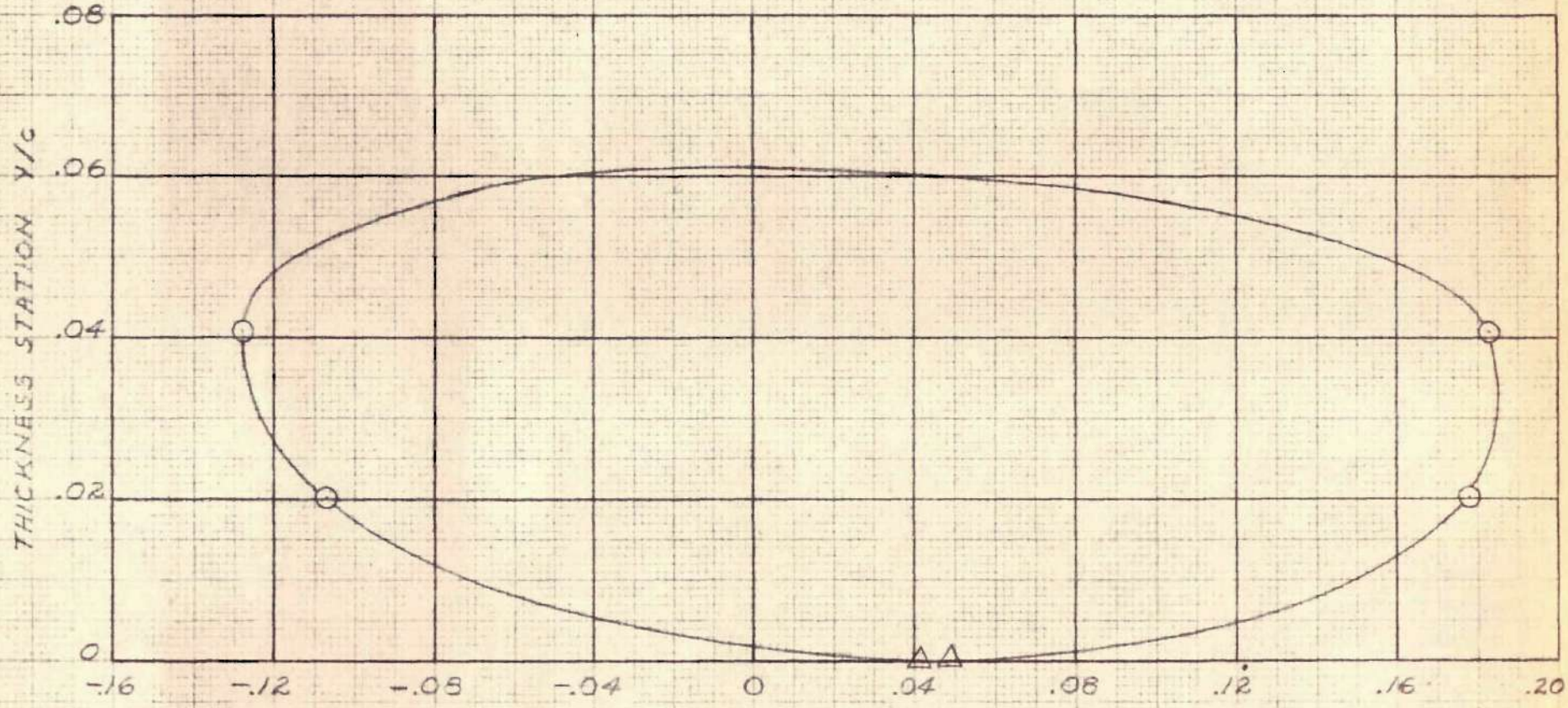

FIGURE 17.- THICKNESS PRESSURE DISTRIBUTION FOR SINGLE PROFILE AT $M = 2.03$, $\alpha = 0°$

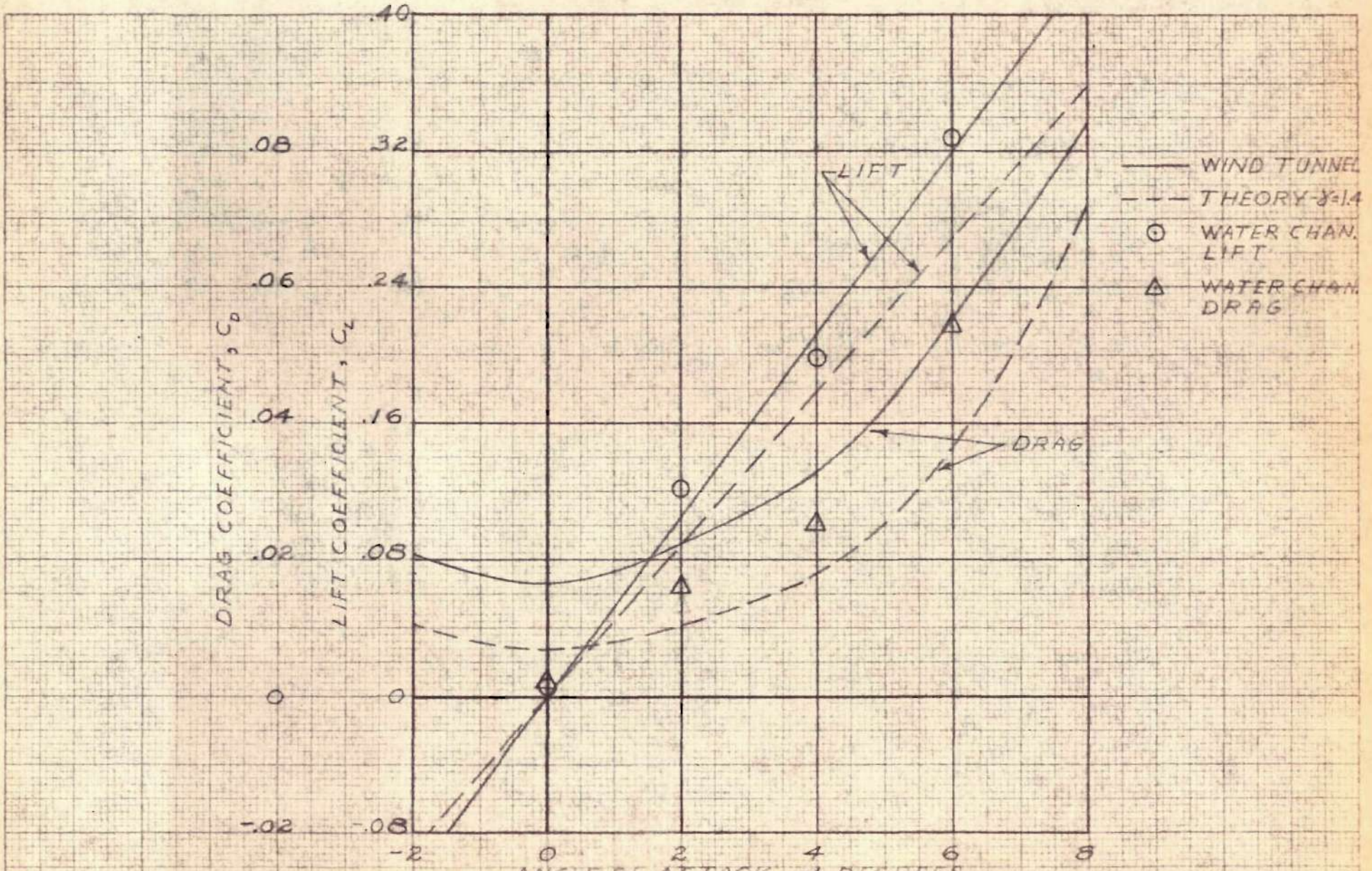

FIGURE 18. – LIFT AND DRAG CURVES FOR BIPLANE AT DESIGN GAP, M = 2.03

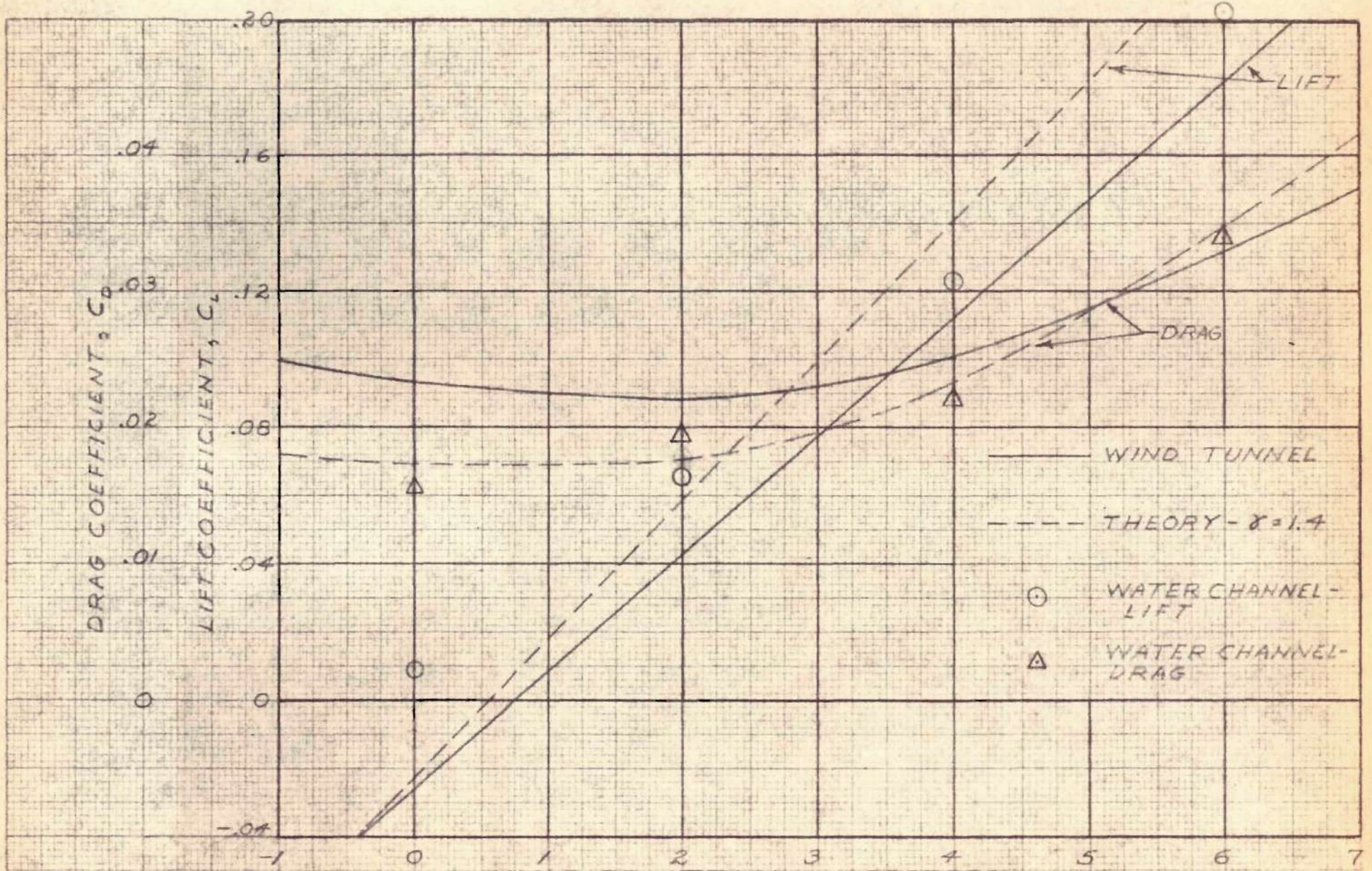

FIGURE 19. - LIFT AND DRAG CURVES FOR SINGLE BIPLANE PROFILE AT M = 2.03

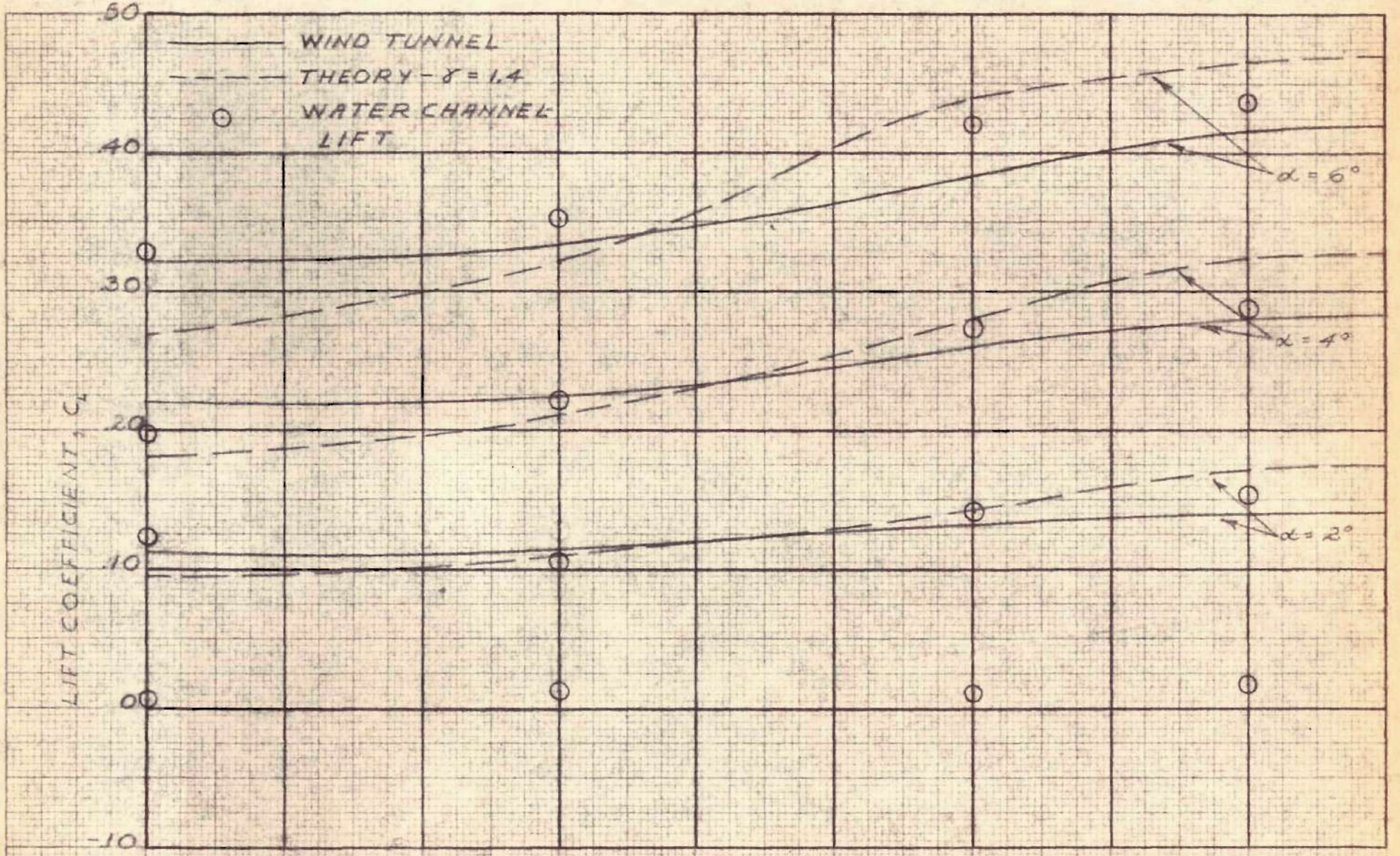

FIGURE 20. - VARIATION OF LIFT WITH BIPLANE GAP RATIO, M = 2.03

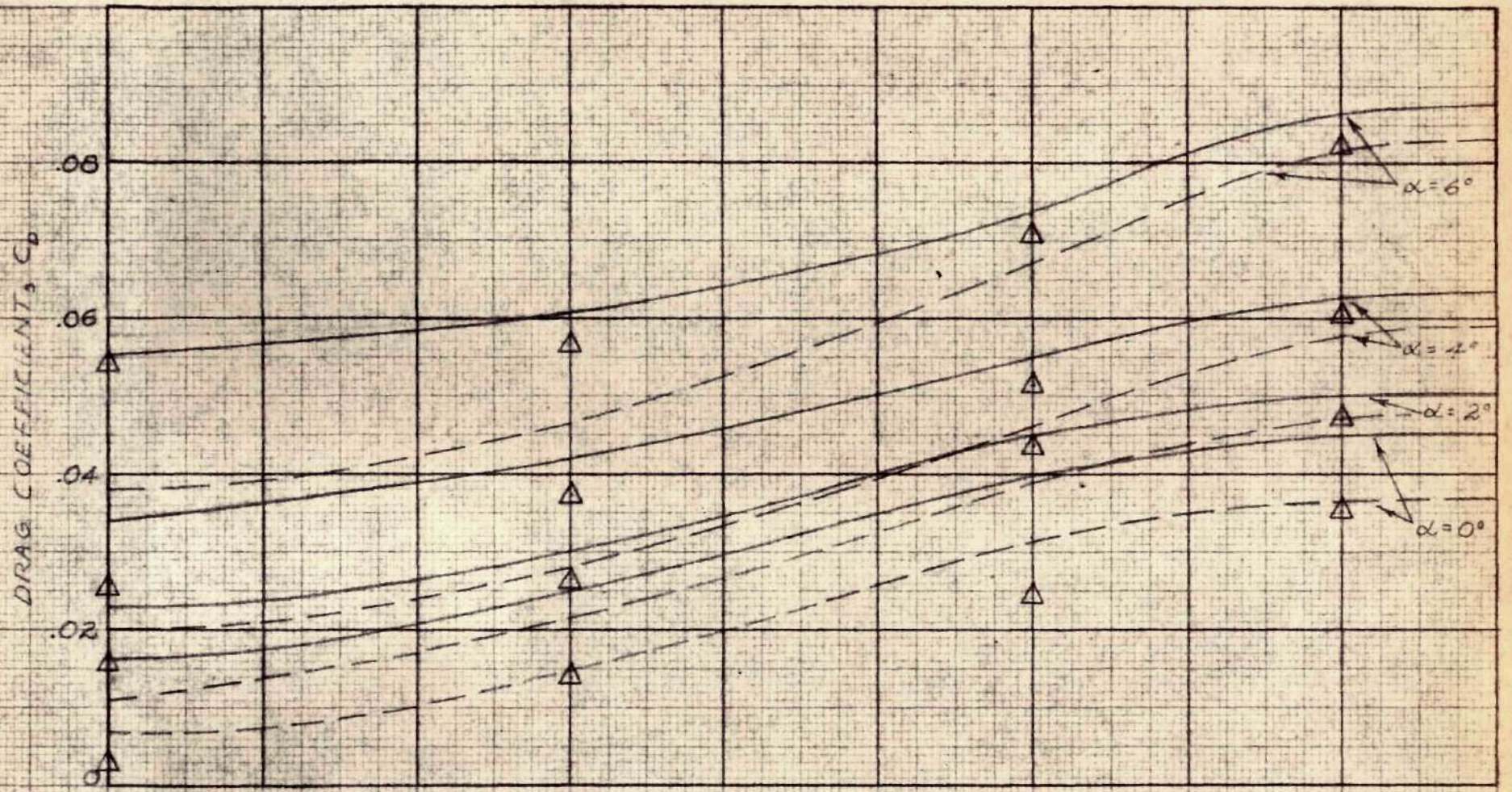

FIGURE 21. - VARIATION OF DRAG WITH BIPLANE GAP RATIO, M = 2.03

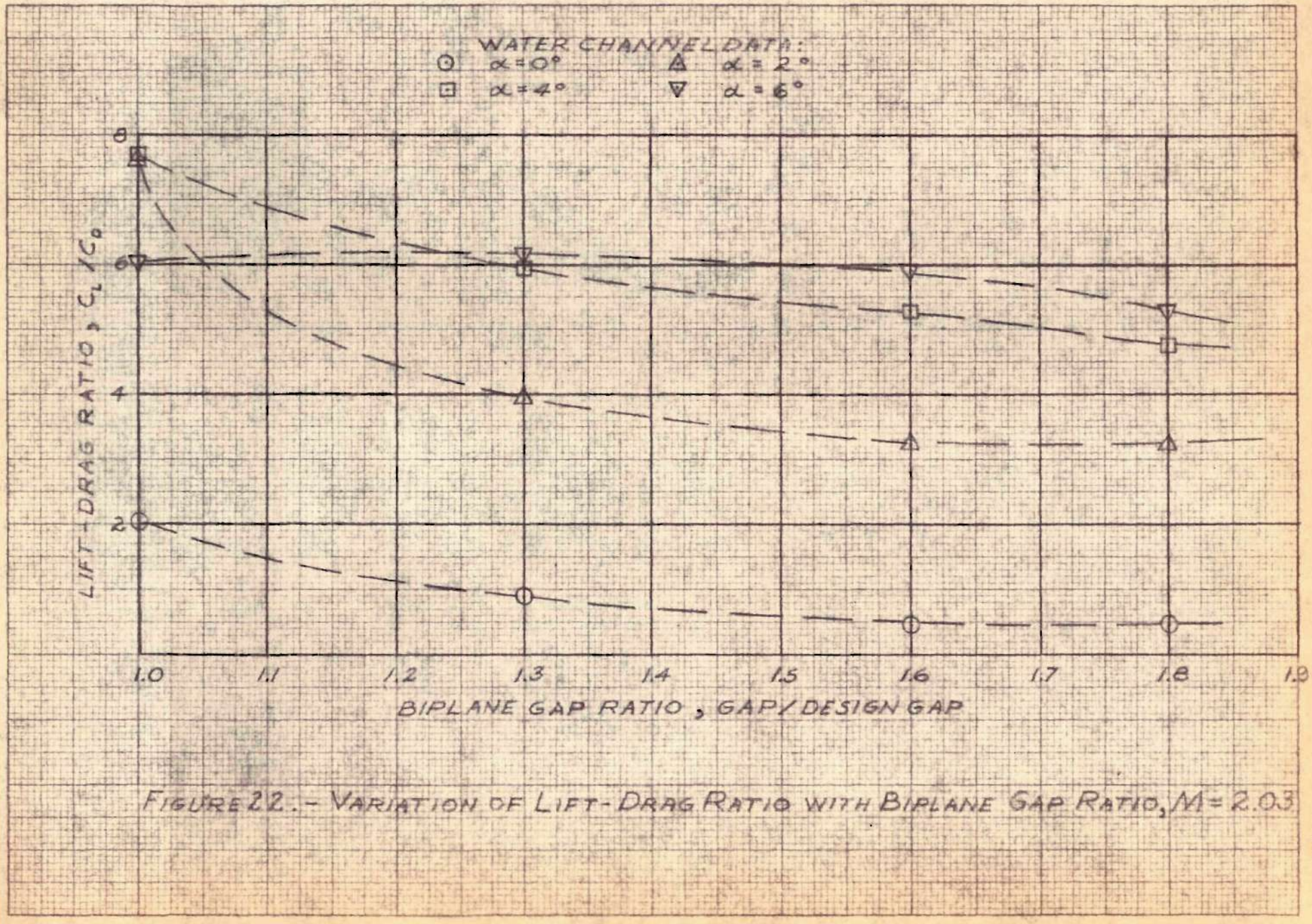

FIGURE 22.- VARIATION OF LIFT-DRAG RATIO WITH BIPLANE GAP RATIO, M = 2.03

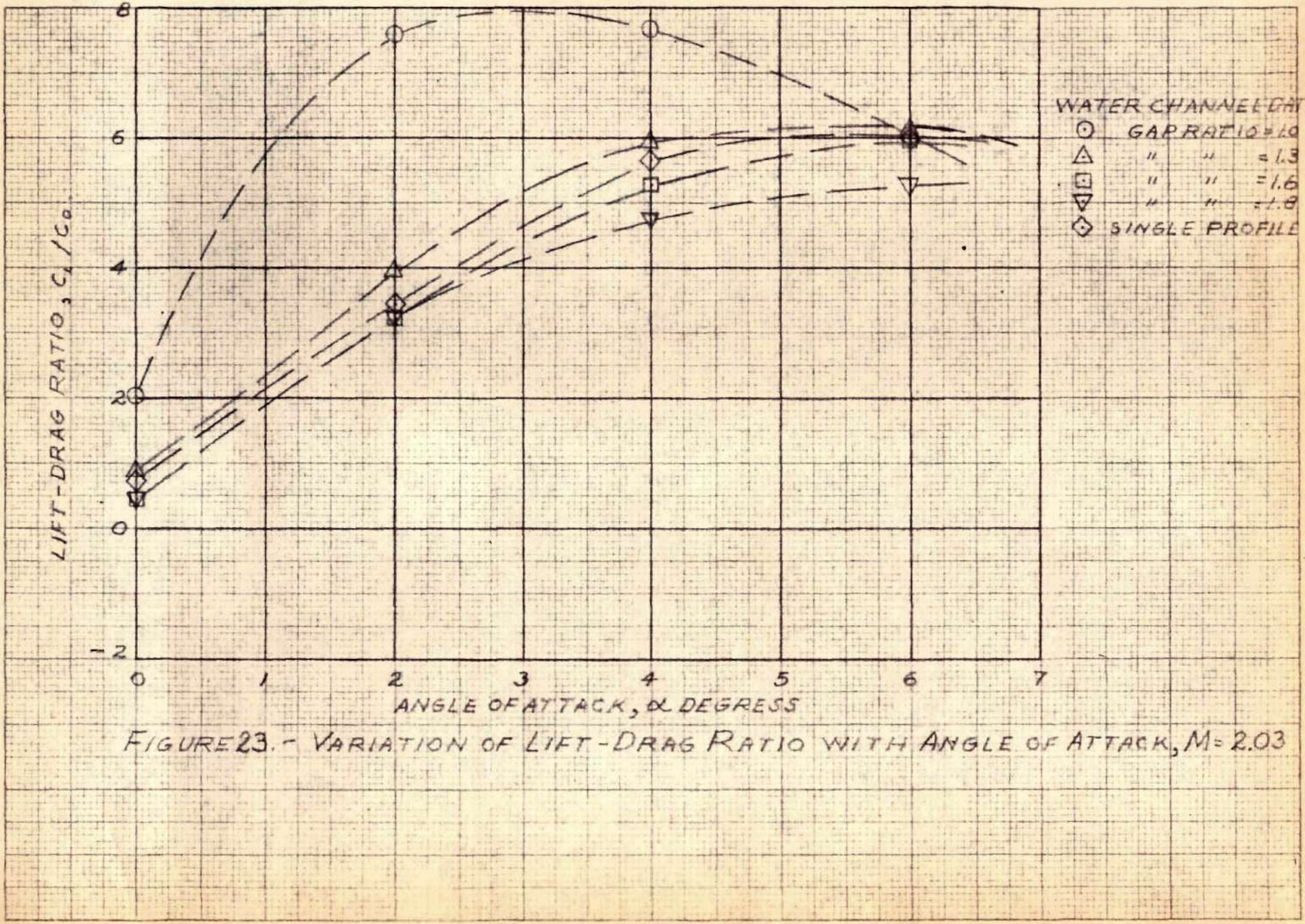

FIGURE 23. - VARIATION OF LIFT-DRAG RATIO WITH ANGLE OF ATTACK, M = 2.03

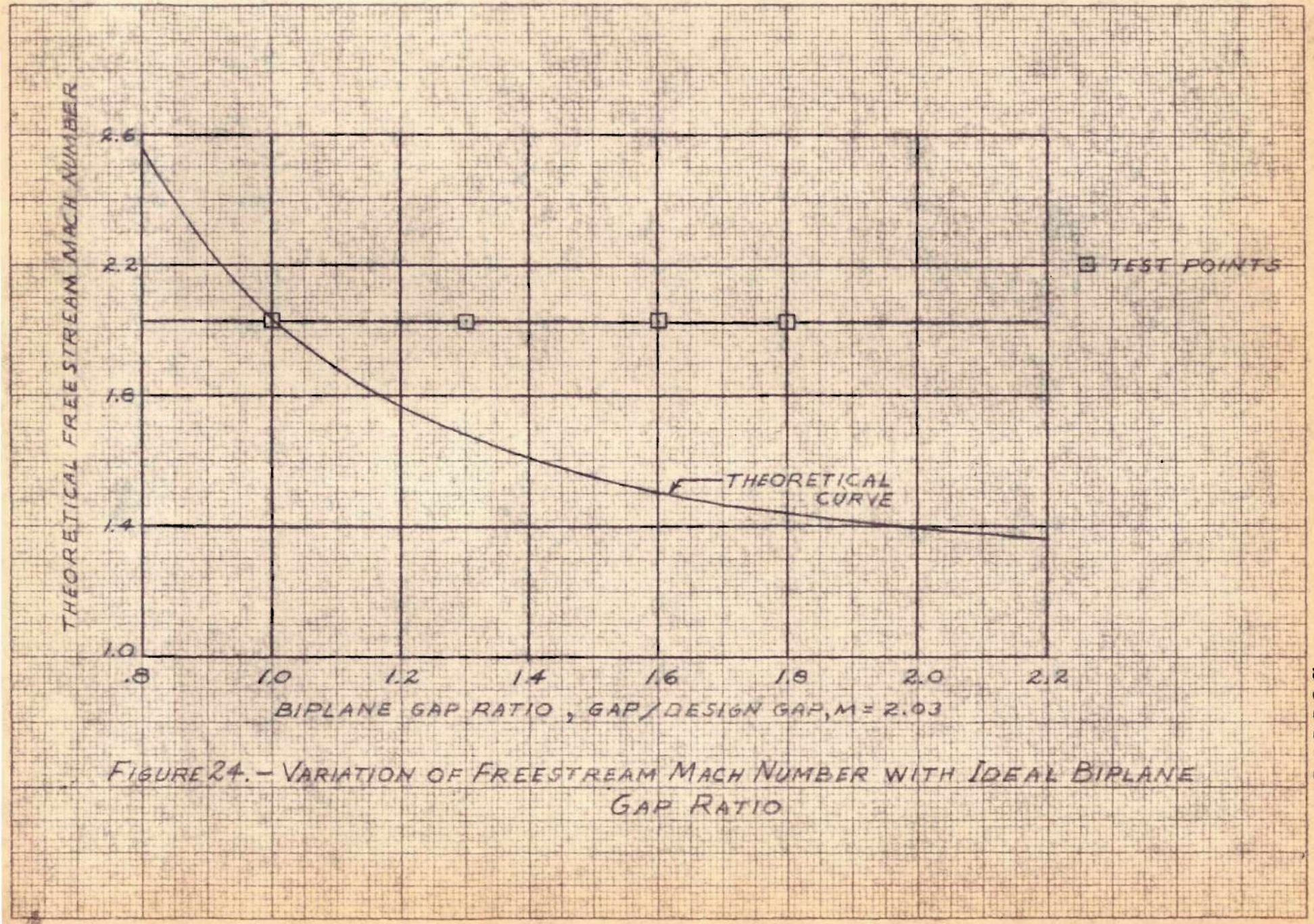

FIGURE 24. – VARIATION OF FREESTREAM MACH NUMBER WITH IDEAL BIPLANE GAP RATIO